Perfusion and Metabolism Imaging Studies In Parkinson's Disease

- with special reference to intensity normalization methods

Per Borghammer, MD, PhD, DMSc

This review has been accepted as a thesis together with seven previously published papers by Aarhus University March 22nd 2012 and defended on April 20th 2012.

Official opponents: Ian Law, Copenhagen, and Alain Dagher, Montreal.

Correspondence: Department of Nuclear Medicine and PET center, bygn. 10, Aarhus University Hospital, Noerrebrogade 44, 8000, Aarhus, Denmark.

E-mail: per@pet.auh.dk

Dan Med J 2012;59(6): B4466

THIS DOCTORAL THESIS IS BASED ON THE FOLLOWING PEER-REVIEWED PUBLICATIONS.

I: **Borghammer P**, Jonsdottir KY, Cumming P, Ostergaard K, Vang K, Ashkanian M, Vafaee M, Iversen P, Gjedde A. (2008) Normalization in PET Group Comparison Studies – The Importance of a Valid Reference Region, NeuroImage. Apr 1;40(2):529-40.

II: **Borghammer P**, Cumming P, et.al. (2009). Artefactual subcortical hyperperfusion in global mean normalized PET studies: Lessons from Parkinson's disease. NeuroImage. Apr 1;45(2):249-57.

III: **Borghammer P**, Aanerud JA, Gjedde A. (2009). Data-driven intensity normalization of PET group comparison studies is superior to global mean normalization. NeuroImage. Jul15;46(4): 981-8.

IV: **Borghammer P**, Cumming P, Aanerud JA, Förster S, Gjedde A. (2009). Subcortical elevation of metabolism in Parkinson's disease—a critical reappraisal in the context of global mean normalization NeuroImage. Oct 1;47(4):1514-21.

V: **Borghammer P,** Østergaard K, Cumming P, Gjedde A, Rodell A, Hall N, Chakravarty MM. (2010). A deformation-based morphometry study of patients with early-stage Parkinson's disease. Eur J Neurol. 17(2):314-20.

VI: **Borghammer P**, Chakravarty MM, Jonsdottir KY, Sato N, et.al. (2010). Cortical hypometabolism and hypoperfusion in Parkinson's disease is extensive – probably even at early disease stages. Brain Structure and Function. 214(4):303-17.

VII: **Borghammer P**, Hansen SB, Chakravarty MM, Eggers C, Vang K, Aanerud J, Hilker R, Heiss WD, Rodell A, Munk OL, et.al. (2012). Glucose metabolism in small subcortical structures in Parkinson's disease. Acta Neurol Scand. 125(5):303-10

ABSTRACT

Positron emission tomography (PET) and single photon emission computed tomography (SPECT) are important tools in the evaluation of brain blood flow and glucose metabolism in Parkinson's disease (PD). However, conflicting results are reported in the literature depending on the type of imaging data analysis employed. The present review gives a comprehensive summary of the perfusion and metabolism literature in the field of PD research, including (1) quantitative PET studies, (2) normalized PET and SPECT studies, (3) autoradiography studies in animal models of PD, and (4) simulation studies of PD data. It is concluded that PD most likely is characterized by widespread cortical hypometabolism, probably even at early disease stages. Widespread subcortical hypermetabolism is probably not a feature of PD, although certain small basal ganglia structures, such as the external pallidum, may display true hypermetabolism in the absolute sense. This observation is also in agreement with the animal literature.

1. INTRODUCTION

Parkinson's disease (PD) was first described in 1817 by James Parkinson (Parkinson, 1817), as a movement disorder characterized by a resting tremor, slowness of movement, muscular rigidity, and postural instability. In addition, non-motor manifestations (Langston, 2006), including hyposmia (Doty et al., 1992), and autonomic and cognitive deficit (Kehagia et al., 2010), are increasingly recognized as being part of the clinical syndrome. Indeed, more than 30% of patients eventually develop dementia (Aarsland and Kurz, 2010). Initially, PD was believed to be primarily a disorder of the dopamine system. However, comparable levels of cell loss are seen in other neurotransmitter systems, including the noradrenergic (Gai et al., 1991) and cholinergic (Chan-Palay, 1988) systems. At later disease-stages, widespread α–synuclein pathology and neuronal loss is present in the cerebral cortex (Braak et al., 2003).

Several successful animal models of PD were developed (Cannon and Greenamyre, 2010), most notably the 6-hydroxydopamine (6-OHDA) rodent model (Uretsky and Iversen, 1970), and the 1-methyl-4-phenyl-1,2,3,6-tetrahydropyridine (MPTP) primate and rodent models (Burns et al., 1983). These models have been extensively investigated using various techniques including electrophysiology, immunohistochemistry, and 2-deoxyglucose (2DG) autoradiography (Sokoloff et al., 1977). The latter method allows measuring the metabolic consequences of a dopaminergic lesion, and thence to infer the underlying characteristics of the perturbed neural activity in the parkinsonian basal ganglia. As such, results from the 2DG method were fundamental to the development of the classic basal ganglia circuitry models in

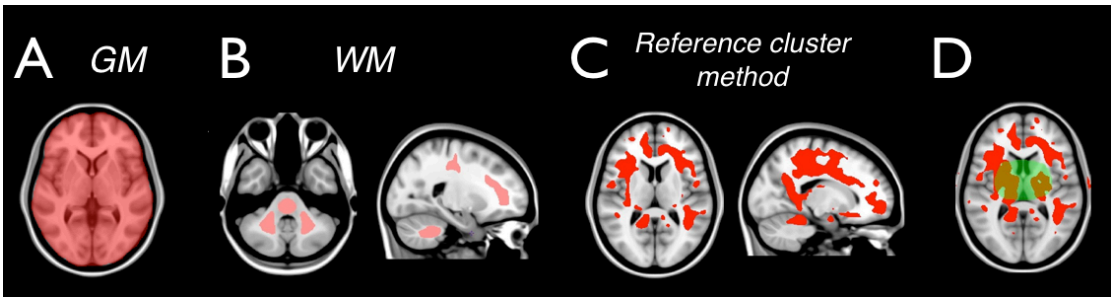

Figure 1

The figure displays three different reference regions used in ratio normalization. **A.** In global mean (GM) normalization, the data is normalized to the mean of all intra-cerebral voxels**. B.** We suggested that central white matter (WM) structures are a better normalization reference in PD and other disorders. **C.** The reference cluster method is an a posteriori normalization approach, in which the reference region is determined from the data per se. The depicted images are derived from a PD vs. controls comparison (VII). First, a standard statistical group comparison is performed using global mean normalization, i.e. with the mask from A. However, from the resultant output t-map only the apparently hypermetabolic voxels (t>2) are included into the final normalization mask (red colored voxels). This region is then used for normalization of the raw data**. D**. The reference cluster method requires that no true increases are present in the patient group. For this reason, central subcortical structures (green outline) must be excluded from the reference cluster in studies of PD, since animal evidence suggest that some of these regions could be truly hypermetabolic. The pattern in C shows the final normalization region after the exclusion of the central voxels.

parkinsonian disorders (Alexander et al., 1990, Mink, 2003, Obeso et al., 2008).

The subsequent development of autoradiography techniques in vivo using Positron Emission Tomography (PET) and Single Photon Emission Computed Tomography (SPECT) have allowed the measurement of the cerebral metabolic rate of glucose (CMRglc), oxygen (CMRO2), and cerebral blood flow (CBF) in human subjects (Valk et al., 2003, Bailey et al., 2005), as well as neuroreceptor availabilities and dopamine synthesis capacity. These imaging methods have been widely used to investigate changes in brain perfusion and metabolism in PD. However, confusing and contradictory results abound in the literature, which make the comparison of different imaging studies of human patients difficult. Moreover, it is vital to firmly establish the similarities and dissimilarities between animal models and the human disorder, since development of novel pharmacological and surgical treatments to a large extent is based upon preclinical testing in animal models. The present review therefore aims to elucidate some of the conflicting evidence and controversies in this literature. A large number of PD studies have been carried out to investigate effects of treatment (Asanuma et al., 2006), disease progression (Huang et al., 2007), and various motor- and cognitive activition paradigms (Lozza et al., 2004). However, in the present review, only studies of the resting state are considered in detail, since obtaining a solid understanding of the nature of the baseline condition seems imperative before more advanced studies of PD can be correctly interpreted.

The Review at a Glance

Sections 2 to 5 mainly contain background material – a necessary prerequisite for understanding our motivation for doing the studies. We realized early on that many of the conflicting results in the semi-quantitative PET and SPECT literature arose depending on the type of data normalization employed in the study. Much of our work was therefore centered on the consequences of different methods of data normalization. In section 2, an account of the most commonly used methods of data normalization is given. The subsequent two sections recapitulate the previous PET and SPECT literature. Section 3 presents the quantitative literature in PD, in which physiological values of perfusion and metabolism were obtained. Section 4 summarizes the studies, in which various types of data normalization were employed. Section 5 ties together the preceding three sections. It is therein demonstrated that the most commonly employed method of normalization, i.e. global mean (GM) normalization, is most likely biased and therefore invalid.

In section 6, we present a series of simulation studies (Borghammer et al., 2008, Borghammer et al., 2009a, Borghammer et al., 2009c), which aimed to elucidate the fitness and capabilities of different types of data normalization in PET studies. Section 7 summarizes the findings from several real-data comparisons of PD patients to healthy controls (Borghammer et al., 2010a, Borghammer et al., 2012), in which the effects of differing methods of normalization were investigated. Section 8 provides the results from a high-resolution PET study of PD patients (Borghammer et al., 2012). Evidence from the animal 2DG literature suggests that real hypermetabolism in PD may only be found in certain very small subcortical structures – too small to be investigated with clinical PET scanners. This study therefore aimed to investigate similarities between human patients and the animal literature using a scanner with sufficient resolution. Section 9 briefly summarizes some of the MRI literature in PD, since the issue of partial volume effects must always be considered in the context of PET studies, especially when brain atrophy is an issue. The results of our MRI study (Borghammer et al., 2010b) are presented. Finally, section 10 provides a discussion.

2. NORMALIZATION OVERVIEW

Although normalization is often employed as a matter of convenience, the ultimate purpose of perfusion and metabolism PET studies has always been to allow absolute quantification of physiological measurements, since CBF and CMRglc are surrogate markers of neuronal activity. The details of the neurovascular and neuroenergetic coupling are complex and yet to be fully resolved (Attwell and Iadecola, 2002, Gjedde et al., 2002, Buzsaki et al., 2007, Sirotin and Das, 2009). Nevertheless, since glucose and oxygen are consumed in stoichiometric quantities to sustain ion gradients across neuronal cell membranes (Attwell and Iadecola, 2002), the metabolic signal recorded by PET is best understood in absolute terms. However, it was realized early on that quantitative PET measurements were not without problems (Di Chiro and Brooks, 1988). As summarized by Alavi and colleagues , the substantial variation present in global CBF and CMRglc values stems from several distinct sources (Alavi et al., 1994):

(1) Normal biological variations in CBF and CMRglc. Intra- and inter-individual variation is introduced by diurnal rhythms of brain activity (Diamant et al., 2002), and other factors such as hemoglobin concentration (Ibaraki et al., 2010), arterial pH, and PaCO2 (Ramsay et al., 1993).

(2) Variations related to instrument performance with regard to measurement of activity concentration in organs and in arterial blood samples (Alavi et al., 1994). Activity in small regions is underestimated due to partial volume effect (PVE) (Hoffman et al., 1979).

(3) Variations related to reconstruction and processing of the acquired images, assigning ROIs, registration of PET to MRI, and calculating physiologic parameters utilizing kinetic models.

Many of these sources of data variation can be minimized and corrected through application of carefully standardized imaging protocols, and post-imaging software correction methods (Valk et al., 2003, Bailey et al., 2005). A full account of these issues is beyond the scope of this review. In the present context, the major point is that a number of known factors add to the considerable variation in the absolute measurements of CBF and CMRglc making difficult the detection of low-magnitude differences. The CBF and CMRglc values in healthy subjects exhibit a coefficient of variance (COV) of 10-20% (Leenders et al., 1990, Wang et al., 1994, Ibaraki et al., 2010), and variances as high as 30% are reported in PD (Huang et al., 2007) and Alzheimer's disease (AD) (Fukuyama et al., 1994). As previously reviewed (Borghammer et al., 2009a), simple power calculations demonstrate that in order to detect between-group differences of 10%, sample sizes of 50-200 subjects per group would be needed (α=0.05, power=90%, COV=15-30%, two-sided test). The impracticability of obtaining such large sample sizes inspired the development of normalization methods to reduce the data variation.

Ratio Normalization

The most commonly used normalization method, termed ratio normalization, involves the computation of the ratio of individual voxel (or VOI) values to the mean of all voxels within a reference region (Buchsbaum et al., 1986, Fox et al., 1988). Three different reference regions are depicted in **Figure 1**. The validity of ratio normalization demands that a proportional relationship exists between the brain voxels of interest and the reference region, i.e. if the reference region is scaled up by 10%, so is every voxel of interest. Thus, the 10% variance, which is assumed to represent irrelevant noise, is removed by ratio normalization. The existence of a proportional relationship has been demonstrated for a number of global scaling factors such as blood gas levels (Ramsay et al., 1993). Another prerequisite for valid ratio normalization is that no between-group differences exist in the reference region. For instance, if a group of patients exhibit a mean 10% decrease in the reference region when compared to controls, a subsequent ratio normalization will result in an apparent relative increase of 11% (1/0.9=1.11) in any patient brain voxel, in the absence of any real physiological alteration in that structure. This simple arithmetic fact constitutes the most important point raised in the present review of the PD literature.

By far the most commonly used reference region is a whole brain (WB) VOI, which includes all intracerebral cerebral grey matter and varying amounts of white matter (Fox et al., 1988). This type of normalization is often termed global mean (GM) normalization or proportional scaling to the GM (**Figure 1A**). We have advocated that biased ratio normalization to the global mean has led to the many reports of widespread cerebrometabolic and perfusion increases in PD (Eidelberg et al., 1994, Imon et al., 1999, Nagano-Saito et al., 2004, Huang et al., 2007) and likewise in many other disorders (Borghammer et al., 2008). We shall return to this point in more detail in section 5. For now, the crucial point is that unbiased ratio normalization in a comparison between patients and control subjects, necessitates the identification of a reference region, where physiology is unaffected by the disease process. For instance, Minoshima and colleagues proposed that the pons was the least affected structure in FDG studies of AD (Minoshima et al., 1995, Vander Borght et al., 1997, Choo et al., 2007, Jokinen et al., 2010). However, the small size of the pons could make it vulnerable to random noise and thus imprecision in the normalization reference. Other investigators have used the cerebellum as a reference region in AD (Soonawala et al., 2002) and PD (Derejko et al., 2006). But the cerebellum in its entirety may also be a suboptimal reference in PD, as several quantitative studies reported absolute cerebellar decreases of CBF (Leenders et al., 1985, Imon et al., 1999) and CMRglc (Sasaki et al., 1992).

We proposed the use of central white matter (WM) structures ((Borghammer et al., 2008, Borghammer et al., 2010a, Borghammer et al., 2012); **Figure 1B**) as a possible unbiased reference region, since no quantitative studies of PD have reported absolute decreases in WM (reviewed in (Borghammer et al., 2008, Borghammer et al., 2010a)). Moreover, the central WM structures, such as centrum semiovale, the pons, and central cerebellar WM often appear relatively hypermetabolic in GM normalized studies (see Figure 1 of (Borghammer et al., 2010a)), underscoring that they are probably the most conserved regions. WM normalization has subsequently been used in studies of AD (Firbank et al., 2011) and other disorders.

Other a priori Normalization Methods

The present review mainly focuses on ratio normalization, since this is the most commonly used method. Other methods were extensively examined and reviewed elsewhere (Fox et al., 1988, Friston et al., 1990, Arndt et al., 1991, Gullion et al., 1996), and will be mentioned only briefly. Friston and colleagues developed ANCOVA normalization mainly for the activation study paradigm, but it has also been used in PD group comparisons (Eckert et al., 2005). In contrast to ratio normalization, which requires absence of real group differences in the reference region, ANCOVA normalization requires the coexistence of homogeneous regression coefficients among the groups (Friston et al., 1990). However, covariance adjustment with gCBF as a covariate can reveal heterogeneous regression coefficients among groups of subjects (Devous et al., 1993; Gullion et al., 1996), which presents a serious limitation to the use of ANCOVA as an approach to removing intersubject variation in gCBF. Also, we demonstrated that ANCOVA normalization with global CMRglc as a covariate introduced artifactual subcortical increases in healthy aging (see supplementary Figure 2 in (Borghammer et al., 2008)), and similar patterns were seen in PD (Eckert et al., 2005).

Another normalization method is implemented in an automated voxel-based algorithm based on the scaled subprofile model (SSM) developed by Moeller et al. (Moeller et al., 1987). The SSM method makes use of log-transformed data, and then performs a "double global mean" normalization, i.e. each subject's data is centered both to the subject's own mean and further centered to the mean of the whole group of subjects (Spetsieris et al., 2006).

Nevertheless, this normalization method is quite similar to the ratio GM normalization described above, and as we shall see, has similar consequences for the subsequent data analysis.

Data-Driven Normalization

In contrast to a priori defined reference regions, methods have been devised to identify a suitable reference region in a data-driven a posteriori fashion. One iterative procedure was proposed by Andersson (Andersson, 1997), to ensure independence between the estimated gCBF and changes in local flow. In the first iteration, a standard voxel-based statistical analysis with GM ratio normalization is performed. The output t-map is used to define a new normalization reference region by including only voxels with t-values close to zero (i.e. -2<t<2). In the second iteration, the original data is now normalized to the new reference region, and another voxel-based analysis is performed. A new reference region is constructed from the second iteration output t-map by again masking only the voxels where t is close to zero. This reference region is used for normalization in the third iteration – and so forth. The reference region usually stabilizes after 3-5 iterations.

In a simulation study (Borghammer et al., 2009a), we demonstrated that the Andersson normalization probably outperforms standard GM normalization in group comparisons of patients to controls. This finding is presented in section 6. However, we also explained how the Andersson method can be inappropriate for in this type of data. In brief, consider an idealized group comparison where one group displays heterogeneous decreases, i.e. one third of the brain is decreased by 20%, one third by 10%, and the remaining third is unchanged. Let us suppose that the global mean is decreased by 10%. The first Andersson iteration yields a t-map, in which the unchanged region appears hypermetabolic (t>2), while only the 20% decreased region will be identified as hypometabolic (t<-2). These regions are excluded in the second Andersson iteration, which retains only the apparently unchanged region (t-values close to zero). However, this region was in reality decreased by 10%, and the subsequent iterations will be identical to the first one. Thus, the Andersson method is trapped in a circularity, and would perform identically to standard GM normalization, since the GM was also 10% decreased. Despite this logical possibility, the iterative procedure actually performed better in the simulation study (Borghammer et al., 2009a), than did GM normalization.

Recently, another data-driven approach was introduced by Yakushev and colleagues (known as the reference cluster method or Yakushev normalization) (Yakushev et al., 2009). The method is similar to Andersson normalization, but involves only two iterations. First, a standard GM normalized voxel-based analysis is performed. In the second iteration, a new normalization mask is likewise defined on the basis of the output t-map from the first iteration. However, the t-map is masked differently, i.e. only "hypermetabolic" voxels are included (**Figure 1C**). Normalization of the original non-normalized data is done with the new mask and the second and final voxel-based analysis is then performed. The valid use of this method requires that the seemingly hypermetabolic region identified in the first iteration, is in fact a conserved region, in which no between-group changes are present. It is assumed that the "hypermetabolic" region has been artificially inflated by biased GM normalization, due to isolated cortical decreases in one group. Upon consideration, we have argued (Borghammer et al., 2009a) that a liberal threshold of t>2 (p<0.05, uncorrected) is preferable to the more restrictive p<0.05 (family wise error corrected) threshold used by Yakushev, since a larger reference region is identified. In section 6, we present results demonstrating that this reference cluster normalization performs extraordinarily well.

Importantly, the reference cluster method can be used even if true hypermetabolism exists in the data. However, knowledge of the truly hypermetabolic regions must be available a priori, to allow the exclusion of these regions from the final normalization mask. With this in mind, we utilized the reference cluster method in two studies of real PD data (Borghammer et al., 2010a, Borghammer et al., 2012). Here, we excluded all basal ganglia and thalamic structures from the final normalization reference region (**Figure 1D**), since a few studies have reported true hypermetabolism in these discrete subcortical structures in animal models of PD (reviewed in (Borghammer et al., 2009b)).

3. QUANTITATIVE STUDIES IN PD

A large number of quantitative PET studies have explored the CBF, CMRglc, and CMRO2 alterations in the brain of PD patients. The methodological approaches of these studies varies a great deal, i.e. the earlier studies were PET only, whereas later studies had co-registered CT or MR scans available for VOI definition. Some studies employed full arterial sampling and others used arterialized venous blood sampling. Different kinetic models were used, i.e. both the autoradiographic model (Sokoloff et al., 1977, Hutchins et al., 1984) and full kinetic modeling for estimation of the CMRglc. Nevertheless, certain shared features emerge across these many studies. The following sections review the global and regional changes in absolute CBF, CMRglc, and CMRO2 values in PD brain.

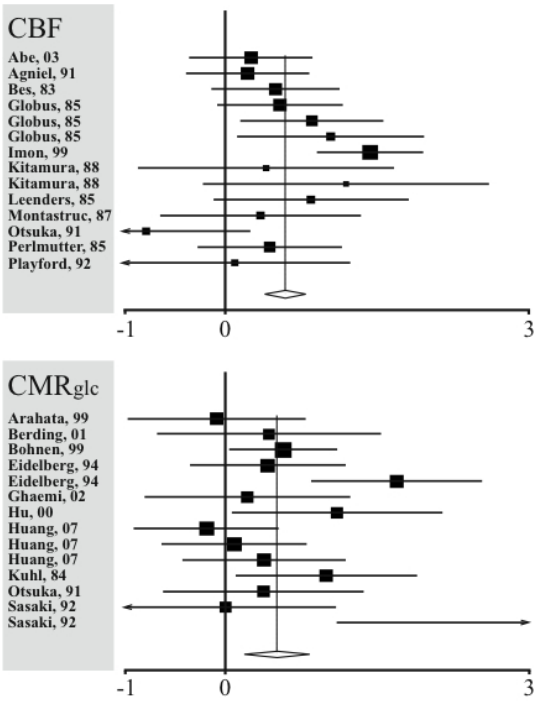

Figure 2

Forest plots of meta-analyses of CBF (top) and CMRglc (bottom) differences between PD patients and healthy controls. Horizontal lines represent 95% CIs around the standard mean difference (SMD) of each study. The size of the squares represent the relative weight assigned to that particular study in calculation of the overall SMD. The vertical lines signifies overall SMD with 95% CI (diamond). [SMD = (between-group difference in mean) / (pooled standard deviation with correction for small sample sizes)]

Global Changes

Global mean values were reported in at least 21 comparisons of PD patients to healthy controls (see Table 2 of (Borghammer et al., 2010a)). Of these, eleven studies reported global CBF values (Bes et al., 1983, Globus et al., 1985, Leenders et al., 1985, Perlmutter and Raichle, 1985, Montastruc et al., 1987, Kitamura et al., 1988, Agniel et al., 1991, Otsuka et al., 1991, Playford et al., 1992, Imon et al., 1999, Abe et al., 2003), ten reported global CMRglc values (Kuhl et al., 1984, Otsuka et al., 1991, Sasaki et al., 1992, Eidelberg et al., 1994, Arahata et al., 1999, Bohnen et al., 1999, Hu et al., 2000, Berding et al., 2001, Ghaemi et al., 2002, Huang et al., 2007), and two studies reported global CMRO2 values (Leenders et al., 1985, Kitamura et al., 1988). The numbers do not add up to 21, since a few studies investigated more than one physiological variable.

Of the 21 studies, seven reported significant global decreases in the PD group. Eleven studies reported decreases, which did not attain statistical significance. Three studies reported small, non-significant increases in global values. As explained in section 2, absolute PET measures of metabolism and perfusion contain a great deal of variation. Consequently, an average decrease of e.g. 10% in the patient group will often be below detection threshold when using modest sample sizes. The mean COV of the 21 studies was 17%, and the average sample size was 14 subjects per group. This yields a statistical power of 32% to detect a between-group difference of 10% in the global mean values. In other words, nearly all previous PET studies were substantially underpowered with regards to detecting a group difference of this magnitude. However, the realization that a 10% difference in the global mean robustly introduces bias into a GM normalized analysis ((Borghammer et al., 2009a, Borghammer et al., 2009c) – see section 6), inspired us to perform formal meta-analyses (Borghammer et al., 2010a) of the 21 quantitative PET studies referenced above.

The meta-analyses demonstrated significant global decreases for CBF ($p<0.001$), CMRglc ($p=0.002$), and CMRO2 ($p=0.04$). Forest plots from the meta-analyses are depicted in **Figure 2** In the case of the CBF and CMRglc studies, additional meta-analyses were conducted on subgroups stratified according to medication status. In both the off- and the on-medication studies, significant combined global decreases were still found for both CBF and CMRglc. Thus, global mean decreases are independent of medication status.

In our systematic literature search, we identified 12 additional quantitative studies of CBF or CMRglc in PD, in which only absolute VOI values rather than absolute global values were reported. These were not included in the meta-analyses. However, in ten of these studies, the authors reported absolute cortical and subcortical decreases (Wolfson et al., 1985, Eidelberg et al., 1990, Karbe et al., 1992, Peppard et al., 1992, Eberling et al., 1994, Kondo et al., 1994, Otsuka et al., 1996, Piert et al., 1996, Vander Borght et al., 1997, Mito et al., 2005). The two remaining studies were of quite small group size. In one, the authors reported regional increases of CMRglc (n=4 patients; (Rougemont et al., 1984)). In the other, the authors reported non-significantly increased CMRglc and significantly increased CMRO2 in 12 early-stage PD patients (Powers et al., 2008). Despite the sometimes aberrant findings, had these 12 studies been included in the metaanalyses, the conclusion would have been even more strongly in favor of generally decreased global values in PD.

We did not stratify the studies included in the meta-analyses according to disease stage or duration, but it seems plausible that cortical decreases in perfusion and metabolism progresses with age. However, when examining the 21 studies (Table 2 of (Borghammer et al., 2010a)), there seems to be little correlation between disease duration and effect size. True longitudinal PET studies of PD populations are rare, but Huang and colleagues (Huang et al., 2007) scanned 15 PD patients at baseline (disease

Table 1. CBF, CMRglc, and $CMRO_2$ findings in 26 *non-normalized* studies of PD patients compared to healthy control subjects.

	Non-Normalized					
	Off			**On**		
REGION	CBF	FDG	$CMRO_2$	CBF	FDG	$CMRO_2$
CORTEX						
Motor	○	○(↓)		↓○	↓○	
SMA		(↓)		↓	↓	
Frontal	↓	○↓	○↓	↓○	↓○	○↓
Parietal		↓○	○	○↓	↓	↓
Temporal	↓○	○↓	○	○↓	○↓	
Occipital	○	○↓	○	○↓	↓	○↓
STRIATUM	○↓	○(↓)	○	○↓	↓○	○
Putamen	○	○		○↓	○↓	○↓
Caudate	○	○↓		○↓	○↓	○↓
Globus Pallidus					(↑)*	
Thalamus	↓	○↓		○↓	↓○	○
Cerebellum	↓	○(↓)	○	○↓	○↓	○
White Matter		○	○		○	○

Up arrows (↑), circles (○), and down arrows (↓) indicate general findings of increased, unchanged, and decreased metabolism/perfusion in PD patients. The columns summarize studies in which patients were either off medication for > 12 hours (Off) or on medication at the time of scan (On). In cells containing more than one symbol, the first symbol designates the finding for which the evidence is the strongest, based on the number of studies and sample sizes. Arrows in brackets signify either non-significant trends or findings of ipsilateral/contralateral asymmetries, for which no comparison to a control group was made. * One small study (n=4 patients) showed increased I/C FDG uptake.

duration <2 years, mean H&Y stage 1.2), and again two years later. Ten of the patients were scanned four years after the baseline scan. The group mean declined 5.5% between the baseline and the second scan, and another 7.4% between the second and third scan. Also, several normalized correlation studies demonstrated progressive cortical decreases with increased disease duration or severity (Kapitan et al., 2009). A question of critical importance is how early a detectable decrease in the global mean (and indeed in localized cortical regions) appears in PD. We shall return to this question in more detail in sections 6 and 7, since it is of fundamental importance to how PET studies of early PD are analyzed.

Regional Changes

A detailed review of the regional CBF, CMRglc, and CMRO2 findings in 26 quantitative PET studies of PD was published previously (Borghammer, 2008). The conclusions of the review are summarized in **Table 1**. In brief, the most robust findings are the reports of absolute decreases in the frontal and parietal cortical regions. The temporal cortices seem to be relatively spared. The occipital cortices are probably more affected than the temporal cortex, but less so than fronto-parietal cortices. The thalamus, striatal structures, and cerebellum exhibited unchanged or decreased values. In the few studies investigating white matter structures there was no evidence of altered WM metabolism. As mentioned above, two small studies reported increases in CMRglc almost everywhere (Rougemont et al., 1984, Powers et al., 2008).

To summarize, the quantitative PET literature reveals that PD is characterized by hypoperfusion and hypometabolism in widespread cortical regions, and possibly also in some subcortical structures. The global mean is most likely decreased as demonstrated by the meta-analyses, which invalidates the use of GM normalization. The reports of hypermetabolism in discrete subcortical structures (pallidum, VA/VL, PPN) in animal models of PD have never been plausibly replicated in quantitative studies of PD patients. For several reasons, this is not surprising. The mentioned subcortical structures are very small compared to the final 10-14 mm resolution of nearly all PET studies performed to date. Moreover, most PET studies employed sample sizes of less than 20 subjects per group, and were thus underpowered to detect low magnitude signals of the order of 10-15%. Other factors, such as head movement and less-than-perfect PET to MRI co-registration make detection of small signals even more difficult.

4. NORMALIZED STUDIES IN PD

In the present section, the main findings in PET and SPECT studies in PD are reviewed. The studies are stratified according to which type of data normalization was used. As we shall see, two very different patterns emerge when GM normalization is compared to ratio normalization to the cerebellum or pons.

GM Normalized Studies

Nearly 20 published studies of PD have employed ratio GM normalization (Eidelberg et al., 1994, Hosokai et al., 2009, Abe et al., 2003, Antonini et al., 2001, Hosey et al., 2005, Kikuchi et al., 2001, Mito et al., 2005, Van Laere et al., 2004, Eckert et al., 2005, Nagano-Saito et al., 2004a, Imon et al., 1999, Miletich et al., 1994, Matsui et al., 2005, Mentis et al., 2002, Ghaemi et al., 2002, Kapitan et al., 2009). Some of these were VOI-based analyses, while others were voxel-based analyses with univariate statistical approaches, i.e. Statistical Parametric Mapping (SPM). A detailed review of these findings is available elsewhere (Borghammer, 2008), but the main findings are summarized in **Table 2**. In summary, relative CBF and CMRglc decreases were often reported in parietal and frontal cortex. Decreases in occipital cortex were reported less frequently, and rarely reported in the temporal cortex. Relative increases were disclosed in motor cortex, lentiform nucleus, thalamus, central cerebellum, and white matter.

Table 2. CBF, CMRglc, and $CMRO_2$ findings in 19 *global mean normalized* studies of PD patients compared to healthy control subjects.

	Normalized to Global Mean								
	Off					On			
REGION	CBF		FDG		$CMRO_2$	CBF	FDG	$CMRO_2$
CORTEX									
Motor	[↑]	↑○	[↑]	↑		○			
SMA	[↓]		[↓]	↓		↓○			
Frontal	[↓]	↓○	[↓]	↓		↓○			
Parietal	[↓]	↓○	[↓]	↓		↓○			
Temporal	[○]	○↓	[○]	○↓		○↓			
Occipital	[↓]	○↓	[↓]	↓		↓○			
STRIATUM									
Putamen	[↑]	○↑	[↑]	↑○		↑↓*			
Caudate	[○]	○↑	[○]	○					
Globus Pallidus	[↑]		[↑]	↑		↓*○↑			
Thalamus	[↑]	○	[↑]	○↑		↓*○↑			
Cerebellum	[↑]	○	[↑]	↑		↑○			
White Matter				↑					

Up arrows (↑), circles (○), and down arrows (↓) indicate findings of *relatively* increased, unchanged, and decreased metabolism/perfusion in PD patients. On and Off signifies whether patients were on medication or drug-fasting at the time of scan. Arrows in square brackets indicate results from studies employing the SSM method. *Only one of the 15 studies reported relative subcortical decreases (Van Laere et al., 2004). See Table 3.1 for more explanation of the symbols.

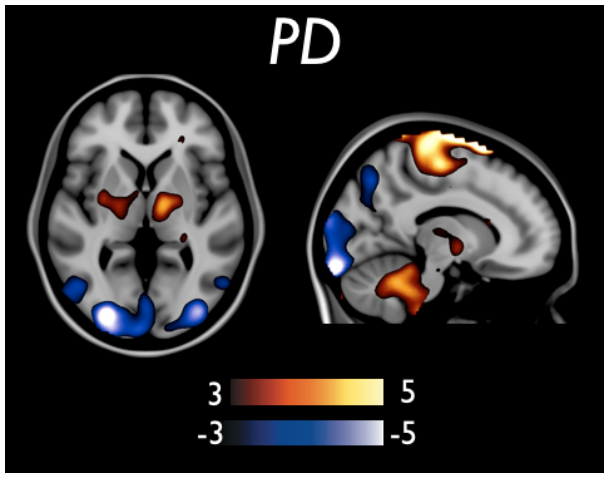

Figure 3
We used the SSM method to compare glucose metabolism in 23 PD patients to 13 healthy controls. Decreases (blue color scale) were detected in frontal and parieto-occipital cortices. Relative increases (hot scale) were seen in white matter, pons, central cerebellum, and the thalamus-capsula interna-lentiform intersection. For visualization the threshold is set at z>3. [Adapted from (Borghammer et al., 2009b)]

The SSM Studies

PET results in a series of papers (Eidelberg et al., 1994, Moeller et al., 1999, Fukuda et al., 2001, Feigin et al., 2002, Lozza et al., 2004, Asanuma et al., 2005, Trost et al., 2006, Huang et al., 2007, Ma et al., 2007, Ma et al., 2009, Poston and Eidelberg, 2010) were analyzed with network principal component strategies using the scaled subprofile model (SSM) method developed by (Moeller et al., 1987, Spetsieris et al., 2006). The main findings are listed in **Table 2** (in square brackets). As explained in section 2, the SSM makes use of a double-GM normalization strategy, which is quite similar to ratio GM normalization. The studies reported a very consistent pattern of relatively increased CMRglc and CBF in putamen, pallidum, thalamus, pons, central cerebellum, white matter, and primary motor cortex. Concomitantly decreased CMRglc and CBF were seen in lateral frontal cortex and lateral and medial parieto-occipital cortex. Using the SSM method (Borghammer et al., 2009b), we also reproduced this pattern in a CMRglc comparison of PD patients to healthy controls (**Figure 3**). The test-retest reproducibility of the pattern is excellent and there is good correspondence between findings in CBF and CMRglc studies (Ma et al., 2007).

VOI Normalized Studies

At least 16 SPECT CBF studies of PD used ratio normalization to the cerebellum (14 studies) or the pons (2 studies) (Pizzolato et al., 1988, Kawabata et al., 1991, Spampinato et al., 1991, Jagust et al., 1992, Sawada et al., 1992, Wang et al., 1993, Markus et al., 1994, Defebvre et al., 1995, Markus et al., 1995, Tachibana et al., 1995, Vander Borght et al., 1997, Arahata et al., 1999, Firbank et al., 2003, Kasama et al., 2005, Osaki et al., 2005, Derejko et al., 2006). These studies were also reviewed previously in detail (Borghammer, 2008), and the main findings are summarized in **Table 3**. In brief, the studies disclosed a pattern similar to that reported in the quantitative studies (compare to **Table 1**), i.e. decreases were seen in fronto-parietal regions and possibly also in occipital and temporal cortices. The pattern of decreases was seen irrespective of patient medication status (on or off medication). Importantly, subcortical relative increases were never reported in any of the 16 studies.

5. GM NORMALIZATION IS BIASED IN PD

Preceding sections show that different PD-related patterns of perturbed metabolism and perfusion are disclosed depending on the method of normalization used. Quantitative studies and studies employing ratio normalization to the cerebellum or pons reveal a common pattern of decreased CBF and CMRglc in cortical regions, and possibly also in subcortical structures. In contrast, studies using GM normalization reveal mostly fronto-parietal decreases with concomitant relative increases in widespread subcortical regions. Since these patterns cannot both be physiologically correct, the question remains which type of normalized

Table 3. CBF, CMRglc, and $CMRO_2$ findings in 16 *cerebellum normalized* studies of PD patients compared to healthy control subjects.

	Normalized to Cerebellum					
	Off			On		
REGION	CBF	FDG	$CMRO_2$	CBF	FDG	$CMRO_2$
CORTEX						
Motor	○				(↓)*	
SMA	○					
Frontal	○↓	○		↓○	↓*	
Parietal	↓○	○		↓○	↓*	
Temporal	○↓	○		○↓	↓*	
Occipital	○	○		○↓	↓*	
STRIATUM	○			↓○	○*	
Putamen	↓	○				
Caudate	↓					
Globus Pallidus	○					
Thalamus	○	○		↓○	↓*	
Cerebellum						
White Matter						

Circles (○), and down arrows (↓) indicate findings of *relatively* unchanged and decreased metabolism/perfusion in PD patients. No studies reported any increases. *Results from a single study of 9 PDD patients, in which the pons was used as a reference region.

findings are representative of real physiological differences in CBF and CMRglc. In the present section, we shall argue that GM normalization is most likely invalid, not only in PD, but also a number of other CNS conditions and disorders. This claim is based on three different lines of evidence, to be summarized below.

Lessons from Quantitative Studies

In section 3, we reviewed that significant absolute global and regional decreases in CBF, CMRglc, and CMRO2 have often been reported in quantitative PET studies of PD. Furthermore, based on meta-analyses of the entire available literature (Borghammer et al., 2010a), we concluded that PD patient groups probably display decreases in regional and hence global values, even if this is not detected in every individual study, due to large inherent variation in the measured physiological values. This makes GM normalization invalid – or at least subject to particular caveats in its interpretation. Nevertheless, real PET data are contaminated by several different types of noise, and it has not been entirely clear what minimal between-group difference in GM values is sufficient to robustly bias subsequent statistical analysis. This question, among others, inspired us to conduct a series of simulation studies (Borghammer et al., 2008, Borghammer et al., 2009a, Borghammer et al., 2009b, Borghammer et al., 2009c), which we shall summarize in detail in section 6. Based on those simulation studies, we demonstrated that a 10% decrease in the GM (and perhaps as little as 5%) robustly produces a pattern of relative increases in structures where no real alteration in CBF or CMRglc occurs. As noted in section 3, previous quantitative PET studies exhibited an average power of 32% to detect a difference of 10% or more. Thus, nearly 7 of 10 studies have not possessed adequate statistical power to detect a decrease in the GM of a magnitude known to invalidate GM normalization. Moreover, most of the GM normalized studies, referenced in section 4, did not acquire quantitative data in the first place and therefore were not amenable for testing whether GM differences were present in their data.

In contrast to the many reports of significant regional and global absolute CBF and CMRglc decreases in PD, absolute increases have never been robustly confirmed. Based on the more than 30 quantitative PD studies performed to date, it seems safe to conclude that the resting state in PD patients is characterized by various degrees of hypoperfusion and hypometabolism in cerebral cortical structures (mostly fronto-parietal), and possibly also in certain subcortical structures. However, the relative subcortical hypermetabolism reported in GM normalized studies have never been confirmed in quantitative data, even though hypermetabolic foci are reported in animal studies using high resolution 2DG autoradiography. Thus, adhering to *lex parsimoniae*, the most probable explanation for the occurrence of widespread subcortical hypermetabolism only in GM normalized studies is that the pattern arises as a product of the GM normalization procedure itself.

Table 4. Disorders in which relatively increased CBF or CMRglc have been reported

Disease	Reference	Increases reported in:
Parkinson's Disease	(Eidelberg et al., 1994, Imon et al., 1999, Nagano-Saito et al., 2004, Asanuma et al., 2005, Huang et al., 2007)	Thalamus, Putamen, GP, pons, Cerebellum, WM
Dementia with Lewy Bodies	(Miyazawa et al., 2010)	Putamen, Cerebellum
Schizophrenia	(Ben-Shachar et al., 2007) (Desco et al., 2003, Buchsbaum et al., 2007)	Putamen, GP, Caudate, Midbrain, Cerebellum, WM
Creutzfeldt-Jakob Disease	(Engler et al., 2003)	Cerebellum, Pons
Hepatic Encephalopathy/ Chronic Liver Disease	(Lockwood et al., 1991, O'Carroll et al., 1991, Ahl et al., 2004)	Thalamus, Putamen, GP, Caudate, Cerebellum, Pons
Wernicke-Korsakoff's Syndrome	(Reed et al., 2003)	Entire WM
DYT1 Dystonia (manifest)	(Eidelberg et al., 1998)	Thalamus, Putamen, Caudate, GP, Cerebellum
DYT1 (non-symptomatic gene carriers)	(Trost et al., 2002)	Putamen, GP, Cerebellum
Posthypoxic Myoclonus	(Frucht et al., 2004)	Thalamus, Pons (tegmentum)
Huntington's Disease (pre-clinical)	(Feigin et al., 2007)	Thalamus, Cerebellum
Progressive supranuclear paresis	(Eckert et al., 2005, Eckert et al., 2007)	Thalamus, putamen, WM
Alzheimer's Disease	(Soonawala et al., 2002, Scarmeas et al., 2004, Habeck et al., 2008)	Cerebellum, WM
Corticobasal Degeneration	(Eckert et al., 2005)	Putamen, Cerebellum, WM
Tourette's syndrome	(Pourfar et al., 2011)	Cerebellum
Narcolepsy-cataplexy	(Dauvilliers et al., 2010)	Cerebellum
Depression	(Kimbrell et al., 2002, Videbech et al., 2002, Perico et al., 2005)	Cerebellum, pons, hippocampus, insula, precentral gyrus
Essential Blepharospasm	(Hutchinson et al., 2000)	Cerebellum, Pons
Healthy Aging	(Moeller et al., 1996, Yanase et al., 2005, Kalpouzos et al., 2007)	Thalamus, Putamen, GP, Cerebellum, WM

Relatively increased CBF or CMRglc have been reported in numerous disorders. All studies used normalization to the global mean. To our knowledge, absolute increases have never been reported in any of these disorders or conditions. [GP=globus pallidus. WM=white matter.]

Common Patterns across Diverse Brain Disorders

Previously (Borghammer et al., 2008), we provided a comprehensive list of brain disorders and conditions, in which subcortical relative increases were reported in GM normalized studies (**Table 4**). The reported increases seem to be confined to a certain set of subcortical regions, i.e. the thalamus-capsula interna-lentiform intersection, pons, central cerebellum, and various WM regions. To demonstrate the similarity between the subcortical relative increases reported in PD studies and patterns seen in other conditions, we performed group comparisons of healthy controls to PD patients ((Borghammer et al., 2009b)); to Alzheimer's patients (AD; (Borghammer et al., 2009b)); and to patients with hepatic encephalopathy (HE; (Borghammer et al., 2008)).

We also compared groups of healthy young to healthy aged subjects (Borghammer et al., 2008, Borghammer et al., 2009b). The patterns of subcortical increases in these other conditions were very similar to the pattern detected in PD patients with GM normalization (**Figure 4**). We hypothesized (Borghammer et al., 2009b) that these phylogenetically ancient subcortical regions (**Figure 5**) are probably more robust than higher-order neocortex, and therefore the subcortical structures could be more conserved across a range of brain disorders. Moreover, compared to the complex anatomical shape of the cerebral cortex, these subcortical structures are geometrically quite simple, which promotes better inter-subject alignment in common stereotaxic space. This would likely tend to decrease variance in the data, and consequently facilitate the detection of any between group differences (even if these were artificially introduced by biased normalization). Nevertheless, the often reported relative hyperactivity in the capsula interna region (see **Figure 4**) could be reinforced by imperfect co-registration, i.e. ventricular atrophy has the propensity to "push" the thalamus more laterally. Thus, unless completely corrected for, the thalamus (grey matter) in patients will be compared to capsula interna (white matter) in controls.

To our knowledge, absolute increases in CBF and CMRglc have never been revealed in any of the disorders listed in **Table 4**. However, in analogy to PD, absolute decreases in regional and global values were reported for most of these conditions. Thus, biased ratio normalization to a decreased GM seems to be the most probable explanation for why such similar patterns of inflated subcortical values are detected across diverse brain disorders.

Discrepancies between Human and Animal Evidence

An extensive review of reported focal changes in brain glucose metabolism in animal models of PD were published previously (Borghammer et al., 2009b). It must be recalled that FDG-PET has a spatial resolution of no better than 5-10 mm, depending on the instrumentation. In contrast, the classical 2-deoxy-glucose (2DG) autoradiographic method (Sokoloff et al., 1977) has an almost cellular resolution of 100-200 μm. A summary of all relevant 2DG autoradiography findings in parkinsonian rats and monkeys is presented in **Table 5**. Two types of findings are presented: (1) comparisons between parkinsonian animals and healthy controls, and (2) changes in the ipsilateral/contralateral ratio of brain regions in hemiparkinsonian animals with unilateral dopaminergic lesions. In the present context of human patient vs. controls comparisons the former contrast is more relevant.

Consideration of these animal studies is complicated by methodological variants in 2DG imaging procedures, and the precise nature of the neurotoxic lesions obtained with MPTP or 6-OHDA. Most importantly, the time interval between intoxication and the autoradiographic procedure ranges from several days to more than a year in the case of some monkey studies. These considerations notwithstanding, results of the 22 published studies show clear consistencies. The resting state for parkinsonian rats and monkeys is mainly characterized by unchanged or decreased glucose consumption in most cortical regions. A few studies revealed small increases in motor-related frontal areas, but even

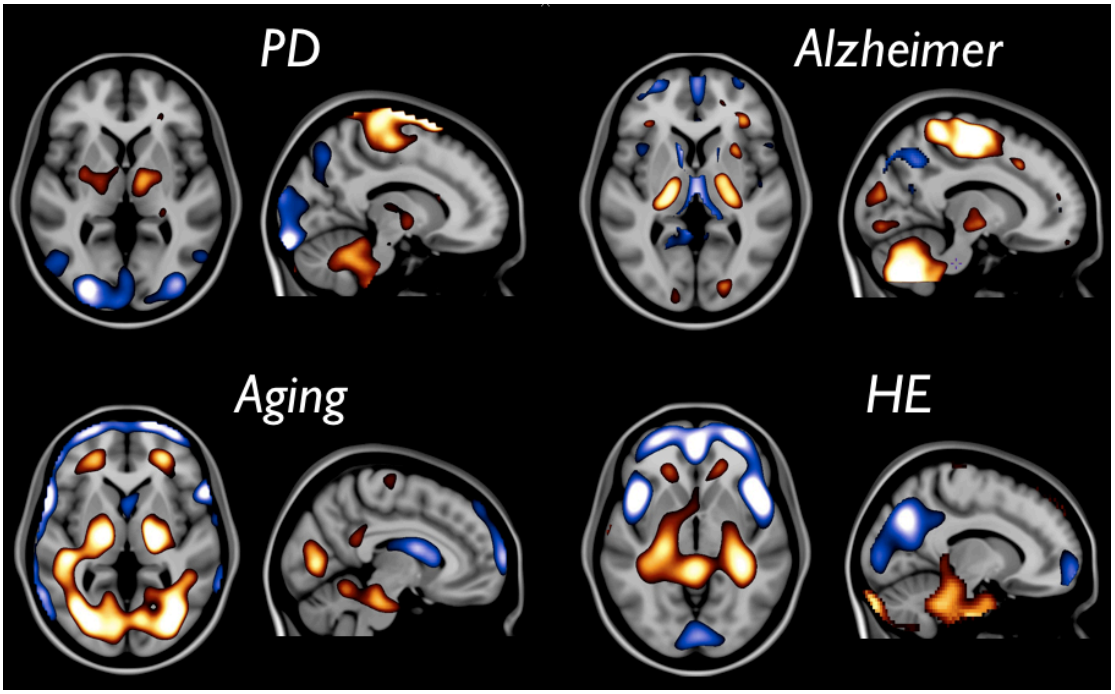

Figure 4

Similar patterns of subcortical relative increases are reported in diverse brain disorders following GM normalization. In the analyses of hepatic encephalopathy (HE) and healthy aging, CBF PET data were used. In the PD and Alzheimer analyses, FDG PET data were used. Blue and hot colors denote significant relative decreases and increases, respectively.

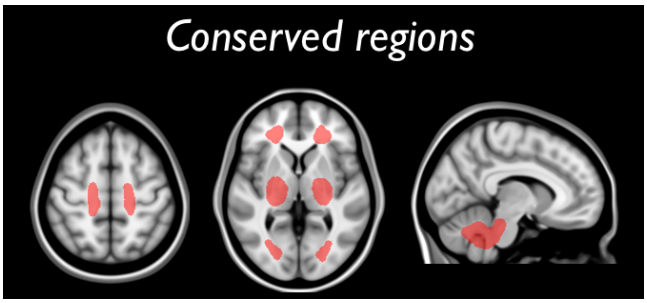

Figure 5
Across a range of brain disorders, a set of subcortical regions appears relatively hypermetabolic when GM normalization is applied. We speculate that these phylogenetically ancient subcortical structures are merely unchanged. Note that the ventricular enlargement often seen in various disease states tends to decrease the PET signal coming from WM and grey matter structures bordering on the ventricles. This would explain why these regions are not often inflated by GM normalization.

more studies showed decreases in the same regions. There is no evidence for hypermetabolism in the white matter, pons, or cerebellum. The subthalamic nucleus (STN) is almost unequivocally hypometabolic. While a few studies suggest striatal hypermetabolism, far more reports suggest unchanged or decreased CMRglc in the parkinsonian striatum. Hypermetabolism in the external pallidum (GPe) and the pedunculopontine nucleus (PPN) is another almost universal finding. While a classic basal ganglia model (Alexander et al., 1990) also predicts hyperactivity in the internal pallidum (GPi), the ventral-lateral (VL), and the ventral-anterior (VA) thalamic nuclei, most animal studies in **Table 5** have shown unchanged CMRglc in these structures.

In summary, robust hypermetabolism were seen only in the GPe and PPN in 2DG autoradiography studies. A few studies suggest possible hypermetabolism in GPi, VA, and the VL, but more studies reported no changes in these regions. The mentioned subcortical structures are all very small, and were most likely below the detection threshold in most human PET studies, in which the final spatial resolution were typically no better than 10 mm (and often worse due to post-scan filtering, head motion, co-registration to standard space). Thus, these subcortical structures can scarcely be examined with clinical PET scanners. Moreover, the many GM normalized PD studies reviewed in section 4 reported relative increases in cerebellum, pons, and WM structures (**Table 2**). Hypermetabolism were never reported in any of these regions in animal models of PD. Of course, it remains certain that toxin-induced animal parkinsonism is different from the human disorder, and that additional real differences in metabolism patterns may consequently exist in PD. Nevertheless, the combined observations that the pattern derived from GM normalized human PET studies do not overlap with the animal evidence, but displays a great deal of overlap with other human disorders, in which no hypermetabolism is expected, strongly suggests that the PD-related relative hypermetabolism arises as a consequence of biased normalization.

We speculated that PD imaging researchers may well have been particularly inclined to accept subcortical relative increases to be indicative of true absolute increases, since the animal literature predicted that such increases should be detected in humans. So these findings of relative hypermetabolism may have been accepted as having face validity, even if they did not exhibit a great deal of overlap with the animal evidence. Similar expectations of hypermetabolism are almost never present for other brain disorders, since many of these do not have representative animal models. Even when animal models are available, subcortical hypermetabolism is rarely reported. Thus, investigators have

Table 5. Summary of 2-deoxy-glucose autoradiography findings in MPTP-monkey and 6-OHDA rat models of Parkinson's disease.

	Decreases		No change		Increases	
	Monkey	Rat	Monkey	Rat	Monkey	Rat
Cortex						
PMC	2,13,17	4 (19)	12,14		18	
SMA	1		12,14		2	
PFC	13,17 (12)	16	11,14,22	20 (5,6,15)	22	
SSC	17,18	4 (3,19)	18			
Visual	13,17	4	12,14,18			
STN	1,9,10,13, 14,17,18,22 (5,12)	3,7 (19)	18	6,20,21		
Striatum	2,13,17,18	4,16 (5,6,19)	1,9,12,14,22	4,11, 20,21 (15)	18,22 (9,12)	
GPe			13		1,7,8,9,10,12, 14,17,18,22	4,20,21 (3,5,6,19)
GPi			9,12,13,14,22	20,21 (19)	1,7,8,17,18	(5,6)
VA	1,18		7,10,14,17,18	3,19 (6)	22 (9,12)	(5)
VL	1,18		9,10,12,14,17	3,19 (6)	7,18,22	(5)
Pf				3,6,19	(12)	
CM			12		9,22	
PPN					3,9,22 (12)	
Pons		(3)	12,14			
Cerebellum	13		2,12,14,17,18			

Summary of studies in which decreases, no change, or increases were reported in parkinsonian animals compared to controls. Numbers in brackets designate findings of ipsilateral/contralateral changes, but in which no comparison to a control group was made. Abbreviations: PMC primary motor cortex; SMA supplementary motor cortex; PFC prefrontal cortex; SSC somatosensory cortex; STN subthalamic nucleus; GPe/i globus pallidus pars externa/interna; VA/VL ventral-lateral/ventral-anterior thalamic nuclei; Pf: parafascicular nucleus; CM: centromedian nucleus; PPN pedunculopontine nucleus [References: 1 (Bezard et al., 2001); 2 (Brownell et al., 2003); 3 (Carlson et al., 1999); 4 (Casteels et al., 2007); 5 (Kozlowski and Marshall, 1980); 6 (Kozlowski and Marshall, 1983); 7 (Meissner et al., 2007); 8 (Mitchell et al., 1986); 9 (Mitchell et al., 1989); 10 (Mitchell et al., 1992); 11 (Mraovitch et al., 1993); 12 (Palombo et al., 1990); 13 (Palombo et al., 1991);14 (Porrino et al., 1987); 15 (Sagar and Snodgrass, 1980); 16 (Schwartz et al., 1976); 17 (Schwartzman and Alexander, 1985); 18 (Schwartzman et al., 1988); 19 (Trugman and Wooten, 1986); 20 (Wooten and Collins, 1981); 21 (Wooten and Collins, 1983); 22 (Gnanalingham et al., 1995)]

not been predisposed to expecting hypermetabolic regions in these disorders.

Interestingly, 2DG autoradiography has gained renewed interest in AD research, due to availability of new and compelling transgenic rodent models (Wisniewski and Sigurdsson, 2010). In this field, the authors seem to have encountered the opposite problem to that described above. Several recent 2DG studies of AD rodent models used GM normalization of the data and reported a flip-flop pattern of hypo- and hypermetabolism (Dubois et al., 2010, Nicholson et al., 2010). These observations do not agree with the extensive human PET literature, in which AD patients do not exhibit true hypermetabolism anywhere in the brain (Herholz, 2010). In AD, as is the case in PD, relative hypermetabolism is only detected when GM normalization is used (Soonawala et al., 2002, Habeck et al., 2008, Habeck, 2010), but here the investigators acknowledge that relative hypermetabolism merely represents an uncontroversial inflation of unchanged regions. Moreover, it was demonstrated that cerebellum normalization is less biased, and in agreement with quantitative PET studies, yields only findings of cortical decreases (Soonawala et al., 2002). This observation also agrees with a previous 2DG study of AD mice, in which investigators used cerebellum normalization and reported only regional decreases in glucose metabolism (Sadowski et al., 2004).

6. SIMULATION STUDIES

Based on the observations and results presented in section 5, we were motivated to conduct several simulation studies (presented in (Borghammer et al., 2008, Borghammer et al., 2009a, Borghammer et al., 2009b, Borghammer et al., 2009c)) with multiple specific aims. First, we investigated the consequences of isolated cortical hypoactivity on subsequent data normalization. In particular, we wanted to estimate the minimum magnitude of cortical hypoactivity propagating robustly to bias, as a consequence of GM normalization. Second, true hyperactivity has been reported in small subcortical structures in animal models of PD. We wanted to determine whether hyperactivity of this magnitude and in analogous structures could plausibly be detected in standard human PET data, using unbiased methods of normalization. Third, late stage PD is characterized by widespread cortical hypoactivity (reviewed in section 3 and 4). However, it seems plausible that similar patterns of widespread decreases could be present in earlier-stage PD, but of such a low magnitude as to preclude detection in PET studies with commonly used sample sizes. For this reason, we investigated the fitness of different types of normalization to detect a spatially extensive pattern of low-magnitude cortical hypoactivity.

Simulations of Isolated Cortical Hypoactivity

The simulation studies all had certain aspects in common. We based the simulation on real CBF parametric images with noise properties and COV in global CBF values comparable to that in previously performed studies. We assembled a pool of 49 quantitative CBF PET parametric images from healthy, adult subjects scanned at our imaging facility. We then randomly sampled two groups of identical sizes, in the first simulation (Borghammer et al., 2008) the groups contained 12 subjects each; in subsequent simulations (Borghammer et al., 2009a, Borghammer et al., 2009b, Borghammer et al., 2009c) the groups contained 20 subjects each. We took measures to match each pair of sampled groups, i.e. we compared the mean age, male/female ratio, and global CBF values of the groups. If any p-value was below 0.50, one group was discarded and a new group was sampled until all p-values satisfied the designated threshold. This procedure resulted in the production of pairs of groups, of very similar composition with respect to in age, gender, and global mean CBF distribution.

The groups were now randomly assigned to become either the control group or the simulated patient group. The latter group of CBF images (in standard space) was now manipulated by multiplying each CBF image with a mask (i.e. template) in standard space.

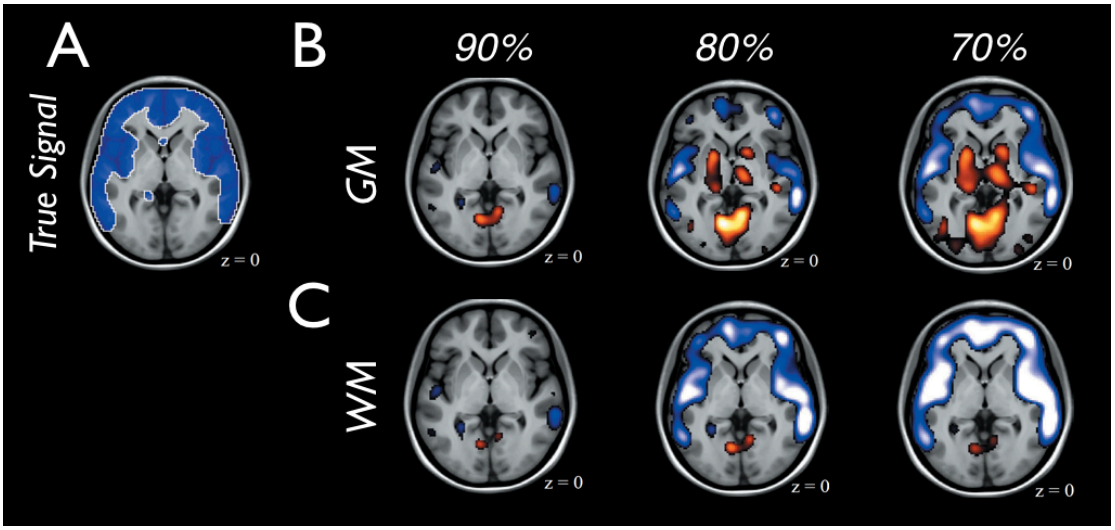

Figure 6
The first simulation (Borghammer et al., 2008) compared the CBF images of two groups of 12 subjects. One group served as controls. The other group had their CBF images manipulated to emulate a uniform fronto-parietal cortical decrease (shown in **A**) to 90%, 85%, 80%, and 70% of original values. Significant relative increase and decreases are depicted with hot colors and blue colors, respectively. **B.** Following GM normalization, progressive decreases in the cortical regions produced increasingly large artificial increases in unchanged regions. Only when the cortical cluster was decreased to 70% of original values did GM normalization reproduce the true pattern of cortical decreases. **C.** Unbiased ratio normalization to central WM produced only negligible relative increases and faithfully reproduced the true cortical pattern of decreased already at the 80% level.

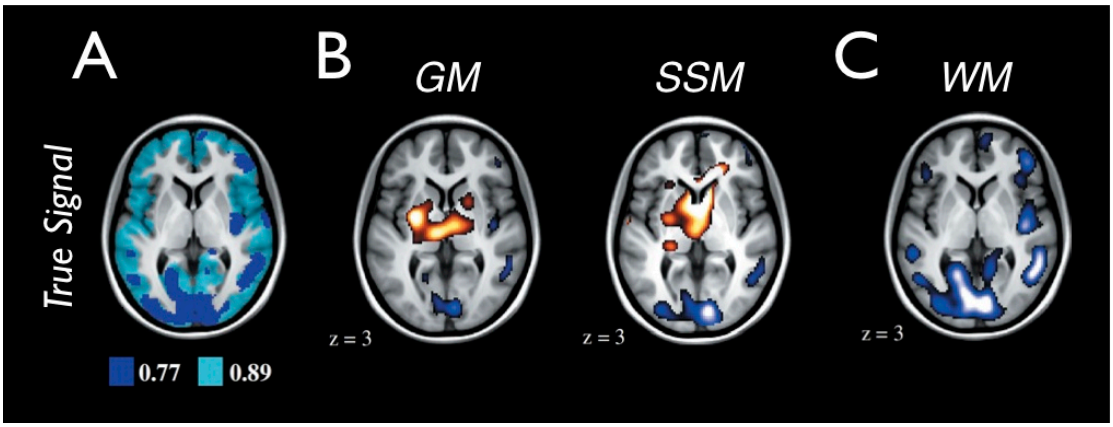

Figure 7

The figure displays results of the first of four repetitions of simulation two (Borghammer et al., 2009c). In this simulation, CBF images of two groups of 20 subjects were compared. **A.** One group had their CBF images manipulated to emulate a hypothetical PD-like pattern of widespread cortical decreases. Large parts of the cerebral cortex were decreased to 89% or 77% of original values. **B.** Univariate analysis with GM normalization and network analysis using the SSM method robustly detected subcortical regions of artificial relative increases. **C.** Unbiased ratio normalization to central WM again recovered more of the true signal. The results were very similar in all four repetitions.

In the first simulation (Borghammer et al., 2008), the mask was designed to emulate the known pattern of cortical decreases seen in healthy aging (**Figure 6A**), i.e. fronto-parietal hypoperfusion. This simulation was repeated four times with four different values in the mask. Thus, by multiplying with the four masks, the fronto-parietal regions of the original CBF images was decreased to 90%, 85%, 80%, and 70% of the original, measured values. All other regions were left unchanged. All CBF images were then blurred with a Gaussian filter to a final 14 mm FWHM, as is conventional for SPM analyses. Finally, voxel-based comparisons were made of the two groups: (a) without normalization, (b) with GM normalization, and (c) ratio normalization to central WM regions, known to be unbiased since the central WM was not included in the manipulation mask.

This first simulation study illuminated several important points, which are of central importance, even if perhaps intuitively obvious. With progressive decreases in the cortical regions, GM normalization produced increasingly large clusters of (artificial) relative increases in unchanged regions (**Figure 6B**). In contrast, GM normalization recovered only little of the true signal imposed by the mask. Ratio normalization to an unbiased region (**Figure 6C**) exhibited the best performance, i.e. recovered most of the true signal, and produced only negligible clusters of relative increases. Importantly, the study demonstrated that a uniform 20% decrease in a large segment comprising nearly half of the neocortex did not result in significant differences in the global mean values, due to the inter-individual variation in global CBF (see Table 3 of (Borghammer et al., 2008)). Thus, had this been a real study, many investigators might have concluded that GM normalization was valid.

In the second simulation of isolated cortical hypoactivity (Borghammer et al., 2009c), we utilized a somewhat more realistic mask (made from the t-map of a previous PD versus controls comparison). The aim was to emulate a plausible PD-like pattern of widespread cortical decreases. Multiplication of the original CBF parametric images with this mask resulted in the decrease of large parts of the neocortex to either 89% or 77% of original values (**Figure 7A**). The magnitude of these values had been first determined by pilot studies. The goal was to impose a reduced GM value in the manipulated group, which would remain statistically indistinguishable in comparison to the unaltered control group. The rest of the preprocessing in this simulation was similar to simulation one, described above, except that 20 subjects per group were used. We repeated the second simulation four times, i.e. with four different samples of groups to test the robustness of the findings. Also, we analyzed the groups with both univariate voxel-based methods and using the principal component network analysis method known as SSM (Moeller et al., 1987). The second simulation (Borghammer et al., 2009c) reproduced the findings of the first simulation. Univariate analysis with GM normalization

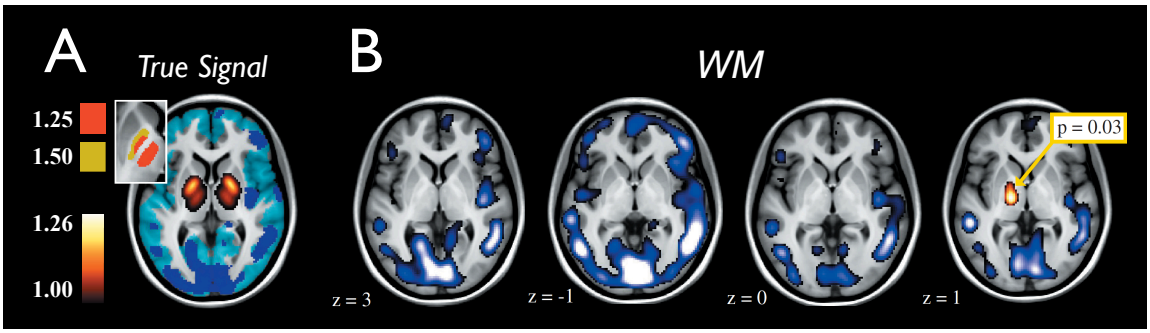

Figure 8

The figure displays results from all four repetitions of simulation four (Borghammer et al., 2009c). **A.** The manipulation mask consisted of the same cortical decreases as in simulation two. Additionally, subcortical structures (see inset) were increased by 50% (GPe), and 25% (GPi, and VA/VL). Following Gaussian filtering the magnitude of the increases was greatly diminished (hot color scale). **B.** Following unbiased ratio normalization to the WM a cluster of significant relative increase (p=0.03) was detected in only one of the four repetitions, and only unilaterally.

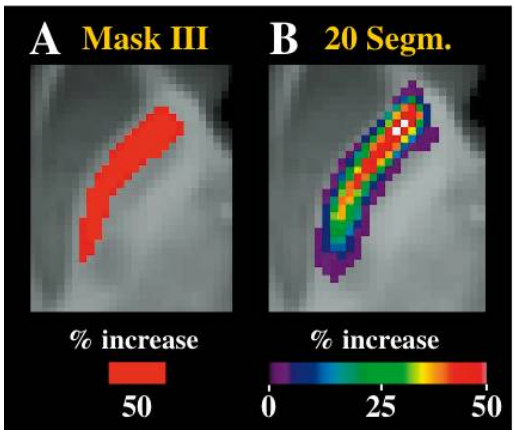

Figure 9

A. The anatomical structures used in the simulations were segmented only once on a high resolution standard MR brain atlas. In simulation four, the globus pallidus pars externa (GPe) was set at a 50% increase. **B.** When the GPe was instead segmented on 20 individual MR scans, the 50% increase was blurred, due to less-than-perfect co-registration. In the shown image slice only a few voxels were included in all 20 segmentations. Had we used this more realistic approach in the simulation studies, the signal would necessarily have been even harder to detect.

and the SSM method both robustly produced artificial relative increases in unchanged, subcortical regions (**Figure 7B**). There was a definite tendency for the relative increases to be present in the same subcortical regions as reported in PD and many other disorders (see **Figure 4**). Subsequent to univariate analysis with WM normalization, more of the true signal was recovered in all four repetitions of the simulation (**Figure 7C**). In all simulations, there was no significant difference in CBF GM between the controls and the manipulated groups (see Table 1 of (Borghammer et al., 2009c)), despite the larger sample sizes. Thus, once again had it been real data, many investigators might have concluded that GM normalization were a valid strategy.

Simulations of Subcortical Hyperactivity

In the third simulation (Borghammer et al., 2009c), we aimed to investigate whether true hyperactivity in the very small structures implicated by the animal evidence could possibly be detected in human CBF data. Therefore, small regions of subcortical hyperactivity were added to the manipulation mask. Specifically, a 10% increase was added to the GPi, and VA/VL thalamic subnuclei, and a 40% increase were added to the GPe. These magnitudes of increases were based on the average effect sizes reported in the animal literature reviewed in section 5 (**Table 5**). Except for the subcortical increases, simulations two and three were identical. Importantly, the filtering of the subcortical hyperactive regions substantially (but realistically) diminished the recoverable signal due to the small size of these structures (**Figure 8A**).

The GM normalized analyses of simulation three was unimportant, when seen in the light of the results of simulation two. In short, robust subcortical artificial increases were present in all repetitions of the second simulation, where no true increases were in fact present. So, had these been real data sets, there would have been no way of knowing whether the detected subcortical increases were true positive or false positive. Thus, the important part of simulation three was to investigate whether the unbiased WM normalization was able to disclose the true increases in the small subcortical structures. However, this proved not to be the case. In none of the four repetitions of simulation three, did the voxel-based analyses detect clusters of significant subcortical increases.

We therefore proceeded with a fourth simulation, identical to simulation three, except that even larger subcortical increases were introduced. In simulation four, the GPe CBF was increased by 50%, and the GPi and VA/VL by 25%, bringing the increases nearly in line with the most extreme increases ever reported in the animal literature (**Figure 8A**). Nevertheless, in only one of the four repetitions of simulation four was a cluster of significant subcortical increase detected, and this increase was only unilateral, despite the bilateral masking (**Figure 8B**).

We note that these simulations contained a methodological flaw, which, if corrected, would have made the subcortical increases even harder to detect. This point is illustrated in **Figure 9**. In brief, when we created the manipulation mask, we segmented the pallidal and thalamic structures only once – on an atlas brain in common stereotaxic space. We then multiplied the mask with the individual CBF images, also in common space, such that exactly the same volume of voxels was manipulated in all 20 subjects. In other words, this procedure was equivalent to perfect coregistration, which is generally unattainable in true data sets. To illustrate the effect introduced by less-than-perfect coregistration, we segmented the left GPe on the individual MRI scans of 20 subjects (Borghammer et al., 2009c). The MRI scans were then coregistered to common space using linear and non-linear transformations. **Figure 9** illustrates that, even if a uniform 50% increase in the GPe were present in all 20 individuals, this signal would have been substantially eroded by co-registration to common space. Had we chosen this cumbersome but more correct approach, no significant subcortical increases at all would have been detected in simulation four, due to the more realistic erosion of specific signal.

This example serves to illustrate a central point of this review. Very small brain structures are best investigated in native space, since the intra-individual PET-to-MRI co-registration error is smaller than the error imposed by warping all images to common stereotaxic space.

Comparison of a priori and a posteriori Normalization

We demonstrated above that GM normalization is invalid in group comparisons, in which one group has isolated cortical decreases of a certain (minimum) magnitude. Importantly, due to insufficient sample sizes, the GM difference will often evade detection. In this setting, ratio normalization to an unbiased VOI (WM) performed much better. In the last series of simulations (Borghammer et al., 2009a), we additionally compared the performance of those standard ratio normalization methods to data-driven normalization, where the reference region is defined a posteriori.

The general procedure of these simulations was identical to simulation two described above. Again, two groups of 20 CBF parametric images were randomly sampled from the common pool. We performed ratio normalization to the GM (known to be biased), as well as unbiased normalization to central WM structures. Additionally, we performed data-driven normalization with the Andersson (Andersson, 1997), and the reference cluster methods (Yakushev et al., 2009), which were explained in detail in section 2. The results of this, the fifth simulation, are displayed in **Figure 10**.

In brief, the findings from simulation two were reproduced. Standard GM normalization displayed the poorest performance - only a minor part of the true signal was detected (**Figure 10B**). Indeed, of the voxels where the CBF magnitude was decreased to .89 of original values, only 6% were recovered by GM normaliza-

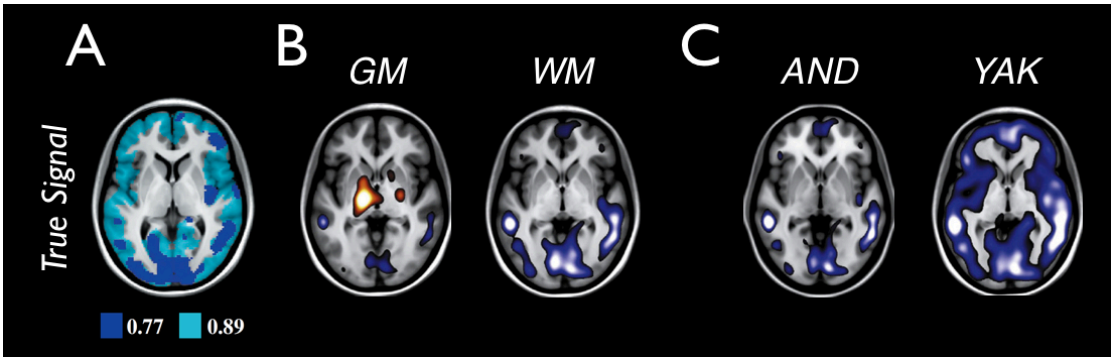

Figure 10
Illustration of four types of normalization used in simulation five (trial 2**). A.** The manipulation image volume was identical to the one used in simulation two. **B.** Following ratio normalization to the global mean (GM) and to central white matter (WM), the findings from simulation two were reproduced – GM normalization detected little of the true signal (but gave rise to artificial subcortical hypermetabolism). WM normalization recovered more of the true signal. **C.** A posteriori normalization was done using the Andersson (AND), and reference cluster method (YAK). Andersson normalization displayed a performance in between GM and WM normalization. The reference cluster method displayed by far the best performance. [Adapted from (Borghammer et al., 2009a)].

tion. Moreover, artificial increases were created. Unbiased ratio normalization to the WM faired a little better (**Figure 10B**). No artifacts were seen in the t-maps, and 33% of the slightly decreased (.89) voxels were detected. The Andersson method did not produce artifacts, and recovered more signal than GM normalization – but less than WM ratio normalization. Finally, the reference cluster method performed extraordinarily well (**Figure 10C**). It correctly identified 65-95% of the slightly decreased (11%), and above 91% of the substantially decreased (23%) voxels. A 3D rendition of the same results is presented in Figure 1A of a previous paper (Borghammer et al., 2010a).

Conclusion and Predictions

Based on the simulation studies summarized above, the three questions posed at the beginning of this section can be addressed. First, we wished to estimate the magnitude of cortical hypoactivity needed to robustly introduce bias, when GM normalization is employed. The brief, but important answer to this question is that significant relative increases robustly appeared in all of the simulations. These increases furthermore appeared in the absence of significant group-differences in absolute GM values. This demonstrates that, unless very large subject samples are available, the absence of absolute global mean differences cannot be relied upon to validate GM normalization. It also demonstrates that biased GM normalization is a plausible explanation for the many reports of widespread subcortical increases in PD and other disorders (see section 4 and 5). As such, we argued that GM normalization should probably be abandoned altogether in any group comparison, in which between-group differences in the GM are suspected to occur. Importantly, such suspicions may only be raised on the basis of a priori knowledge, or following meta-analyses of several previous studies, as we did in the context of PD studies (**Figure 2**). We also argue that, when no a priori information is available about the data, the Andersson method is most likely a more valid approach than GM normalization. This claim was supported by results of the fifth simulation.

Second, we wished to investigate whether the hyperactivity reported in small subcortical structures in animal models of PD could plausibly be detected in human PET data. Based on our simulations, the answer seems to be in the negative. One caveat is that our simulations were done with CBF data, which are intrinsically noisier than are FDG PET data. However, we deliberately designed the simulations in a way that should compensate for this difference in noise properties. In brief, as demonstrated in **Figure 9**, the same volume of voxels was altered in the entire manipulated group to exactly the same extent. As such, our simulations can be viewed as a simple examination of the relationship, i.e. ratio between the mean values of the small (manipulated) subcortical regions and the mean value of the reference regions. We demonstrated that homogenous differences of 25-50% in the pallidum and thalamic subnuclei probably cannot be detected by clinical PET scanners, unless very substantial subject samples are available. To our knowledge, CBF and CMRglc PET studies with such sample sizes have not yet been conducted (Borghammer et al., 2009b).

Third, we hypothesized that late-stage and early-stage PD may be characterized by similar patterns of widespread cortical hypoactivity. However, in the early-stage patients the pattern could plausibly be of low magnitude and therefore below the detection threshold. In summary, the fifth simulation demonstrated that if such low magnitude cortical hypoactivity is present in PD (and this seems highly likely), it will be completely overlooked if GM normalization is used. Unbiased ratio normalization may disclose a minor part of the pattern – an average of 33% of the pattern was detected in our simulations. In contrast, the reference cluster method recovered the majority of the true signal in this type of data. Based on these observations we hypothesized that the reference cluster method could potentially disclose a pattern of widespread cortical hypoactivity in early-stage PD – and not just any pattern, but a pattern resembling that detected in later-stage PD. This prediction is examined in the following section.

7. DATA-DRIVEN NORMALIZATION IN PD

The simulation studies (Borghammer et al., 2009a) demonstrated that only the reference cluster method (Yakushev et al., 2009) was fit to reliably detect a pattern of widespread cortical hypoperfusion of low magnitude. We then proceeded to apply the reference cluster method to real PD data, consisting of both perfusion and metabolism data, i.e. SPECT 99mTc-ethyl cysteinate dimer (ECD) CBF data and PET FDG data sets. Demographic data of the PD patients and control groups are presented in Table 1 of (Borghammer et al., 2010a). In brief, we compared CBF data of 32 early-stage and 33 late-stage PD patients to 60 age-matched con-

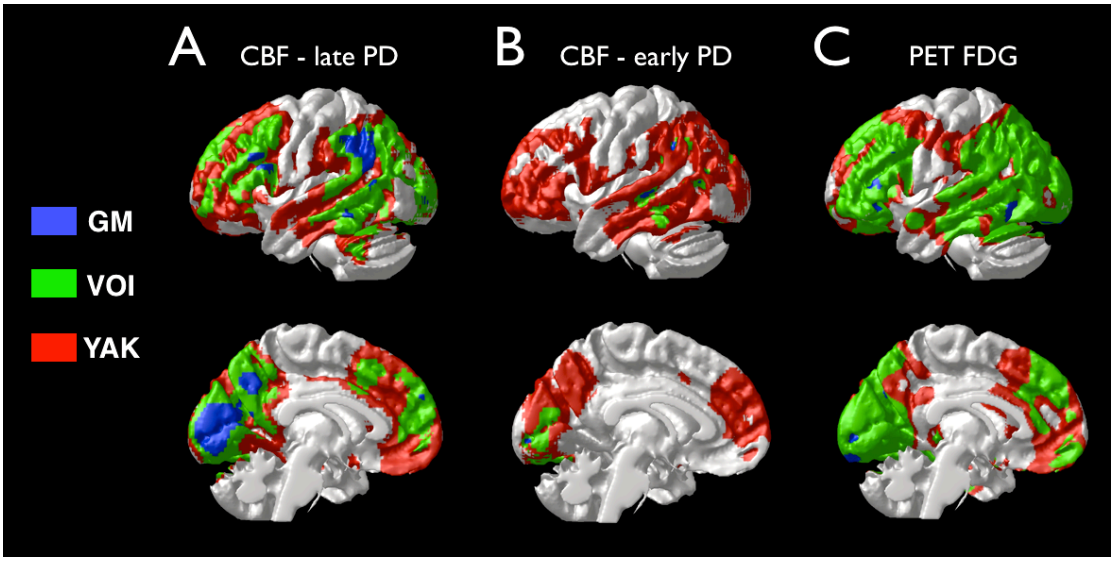

Figure 11
The figure displays the voxel-based comparisons of three PD data-sets (Borghammer et al., 2010). In every comparison three types of normalization were used: global mean (GM) normalization (blue color), ratio normalization to an unbiased volume of interest (VOI; green color), and the reference cluster method (YAK; red color). The different colors on the 3D atlas brain depict the size of the clusters detected following each of the three types of normalization. **A.** SPECT CBF comparison of late-stage PD patients and controls**. B.** SPECT CBF comparison of early PD patients and controls**. C.** PET FDG comparison of moderate- to late-stage PD patients and controls.

trols, and FDG PET data of 23 moderate- to late-stage patients to 13 controls. Voxel-based statistical analyses of the three data-sets were performed subsequent to three different types of normalization: (1) ratio normalization to the GM; (2) ratio normalization to a region encompassing the pons and central cerebellum. These regions were assumed to be unbiased (or at least less biased than GM normalization), since they were previously shown to be unchanged in AD (Minoshima et al., 1995) and PD (Firbank et al., 2003). (3) ratio normalization to the reference region identified by the reference cluster method.

The results of these comparisons are visualized in **Figure 11**. In brief, GM normalization disclosed only small clusters of hypoperfusion and hypometabolism in all three comparisons (blue color in **Figure 11**). These clusters were situated in medial and lateral parieto-occipital cortices and lateral frontal cortices. Ratio normalization to the pontine-cerebellar region disclosed much larger clusters (green color in **Figure 11**), particularly in the late-stage CBF PD data, and in the corresponding PET-FDG data. The spatial extent of these patterns was generally in agreement with previous cerebellum normalized studies (Vander Borght et al., 1997, Firbank et al., 2003, Kasama et al., 2005, Osaki et al., 2005).

The reference cluster method yielded widespread and very similar patterns of cortical decreases across all three comparisons (red color in **Figure 11**). The patterns involved medial and lateral parieto-occipital cortices, lateral temporal lobe, and medial and lateral prefrontal cortices, and anterior cingulate. In all three comparisons, the following structures were unchanged: the medial temporal lobe and temporal pole, sensori-motor cortex, supplementary motor area (SMA), and most subcortical structures including the thalamus, basal ganglia, brainstem, and cerebellum.

In section 8, we provide the results from a high resolution FDG PET study of early- to moderate-stage PD patients. The main objective of that study was to conduct a VOI investigation of small subcortical structures. However, we also performed a voxel-based comparison of PD patients and controls following reference cluster normalization. Also in this patient group, a widespread and very similar pattern of cortical hypometabolism was detected (see Figure 3A of (Borghammer et al., 2012)).

Altogether, these studies suggest that PD may be characterized by more widespread cortical involvement than hitherto believed. We found it particularly striking that early-stage PD patients displayed a nearly identical pattern of hypoperfusion to the patterns obtained from analyzing later stage patients. As such, we argue that our prediction from the simulation studies were confirmed, namely that widespread cortical hypoactivity is present in early-stage PD patients, but that it is below detection threshold when using standard means of data normalization.

The credibility of this claim depends crucially on the validity of the reference cluster method. In short, are the relative differences found by this method equal to true absolute differences? This question is difficult to answer at present, but a number of supporting factors suggest that it may be so. First, in our simulations, the reference cluster method showed a markedly better performance than standard methods. More of the true (quantitative) signal was recovered. No false hypermetabolic voxels were detected, and very little false hypometabolic voxels were detected. Of course, this argument depends on the adequacy of our simulated data. Second, highly similar patterns were detected across four groups of patients (Borghammer et al., 2010a, Borghammer et al., 2012). Such similarity can scarcely arise by coincidence, but must be indicative of underlying commonalities between early- and late-stage patients. Nevertheless, replication of the present results should be carried out in prospective studies.

Third, a similar shift of patterns was reported in very mildly affected AD patients (Yakushev et al., 2009). Using GM normalization only a minor part of the parietal lobe exhibited hypometabolism. However, subsequent to reference cluster normalization, a much larger fraction of the parieto-occipital, temporal, and prefrontal cortices were involved. Moreover, the motor strip and subcortical regions were also largely spared in AD. Fourth, and maybe most importantly, the normalization region obtained by the reference cluster method in studies of PD (and AD) comprises

mainly subcortical regions, i.e. central WM, basal ganglia, thalamus, pons, and central cerebellum (**Figure 1C**). As reviewed in section 3, quantitative PET studies have rarely or never reported absolute changes in these structures, suggesting that they are likely unchanged – and therefore valid as a reference region.

An additional piece of important confirmatory evidence for the above claims was published recently in one of the largest quantitative studies of PD to date. Melzer and colleagues (Melzer et al., 2011) compared 61 PD patients to 29 age-matched controls, using arterial spin labeling (ASL) – a validated quantitative MRI perfusion technique (Williams et al., 1992). The authors used principal component analysis (Spetsieris et al., 2009) very similar to the SSM method. This included the use of "double global mean normalization" as described in section 2. In short, they initially detected a pattern of subcortical relative increases and cortical relative decreases very similar to the previously published PD patterns (Huang et al., 2007, Ma et al., 2007). The pattern was very similar to the pattern shown in **Figure 3**. However, the authors then investigated the absolute perfusion values in this pattern, and found nearly identical levels of absolute perfusion in the two groups in the apparently hyperperfused regions. In contrast, large deficits in absolute perfusion were detected in the cortical regions, which were relatively decreased in the PCA analysis. And importantly, the "in-between regions" which were neither relatively increased nor decreased in the PCA analysis, also displayed absolute decreases in perfusion, but to a lesser extent. This suggests that real PD patient CBF data are actually very similar to our simulated data (**Figure 7A**). Moreover, although the authors did not intend to perform reference cluster normalization, their data nevertheless confirms that the region originally found to be relatively hypermetabolic in a GM normalized analysis, is in fact the most valid normalization reference region; only here the level of perfusion was unchanged.

8. HIGH-RESOLUTION PET STUDIES IN PD

As summarized in section 5, evidence from parkinsonian animal models suggests that subcortical hypermetabolism is found only in highly localized and very small structures such as the pallidum, the PPN, and the VA/VL thalamic nuclei. The most consistent finding has been in the external pallidum. In sections 4 to 6 we presented evidence that the much more widespread pattern of subcortical hypermetabolism reported in the human PET studies – which does not agree with the animal evidence - is most likely a product of biased GM normalization, and simply reflects regions where perfusion and metabolism are conserved, but not really hypermetabolic.

We argue that all but one of the previous PET studies had insufficient resolution for the valid investigation of these structures. Clinical PET scanners currently provide a resolution of no better than 5 mm FWHM, which, as noted above, is further reduced by post-reconstruction filtering. In practice, this often brings the resolution down to 14 mm FWHM. And as noted, head motion and imperfect co-registration to common spaces degrades this resolution even further. As a rule of thumb, PET scanners should not be expected to allow investigation of structures smaller than twice the resolution (Bailey et al., 2005), unless such small structures are extremely signal intensive. In other words, most previous PET studies are not suited to detect signals arising from structures smaller than 20-24 mm. Many of the subcortical structures involved in PD are much smaller than this. For instance, the entire pallidum has a volume of about 2 cm3 (Peran et al., 2009), and measures no more than 6-8 mm across (Talairach and Tournoux, 1988).

These observations led us to initiate a high-resolution FDG PET study of PD patients and controls. We used the brain-dedicated high-resolution research tomography (HRRT) PET system. The system has a resolution of about 2 mm FWHM (de Jong et al., 2007). Moreover, we employed a VOI analysis approach since the transfer of images to common space is bound to decrease the signal in the data (see **Figure 9**). In the only previous HRRT study of PD patients (Eggers et al., 2009), the investigators only employed GM normalization. Furthermore, they compared the patients to a young control group, which makes the use of GM normalization even more problematic, since the GM certainly decreases with normal aging (Borghammer et al., 2008, Kalpouzos et al., 2009). They reported relative hypermetabolism in the pallidum, caudate, putamen, and substantia nigra, but given their use of GM normalization, it is impossible to know whether these findings are indicative of true hypermetabolism or simply just inflation of unchanged regions, caused by biased normalization.

In our study (Borghammer et al., 2012), we compared FDG uptake in 21 PD patients to 11 age-matched controls. We again used three different types of normalization, i.e. GM normalization, normalization to central WM structures, and reference cluster normalization (**Figure 1**). We performed a VOI analysis of several subcortical structures, including internal and external pallidum, thalamic subnuclei, STN, putamen, and caudate. In brief, subsequent to reference cluster normalization, only the external pallidum displayed significant relative hypermetabolism. After WM normalization, significant hypermetabolism was detected in the internal and external pallidum, the right VA/VL nuclei, and also in the putamen. A voxel-based analysis of the reference cluster normalized data was also performed. This analysis disclosed a widespread pattern of cortical hypometabolism, which largely corroborated the previously published patterns (Borghammer et al., 2010a) depicted in **Figure 11**.

In summary, this study was the first report of relative hypermetabolism in data, which were normalized by means other than GM normalization. The finding that the external pallidum displays the most significant level of hypermetabolism is in excellent agreement with the animal literature (**Table 5**). Whether hypermetabolism in the internal pallidum, VA/VL and putamen, which was significant only in WM normalized data, is indicative of absolute hypermetabolism is more debatable. This controversy is actually also in agreement with the animal literature, in which hypermetabolism in these structures were reported in only a few studies. No significant differences were detected in the STN, which was surprising, considering that subthalamic hypometabolism is an almost universal finding in animal models of PD.

For several reasons, we argue that the results of this study are probably more reliable than previously published PET studies. First, we used a PET camera with sufficient resolution to allow investigation of the small structures. Second, an a priori defined VOI analysis was performed, which has higher sensitivity than a voxel-based analysis. Third, we attempted to use non-biased means of normalization. However, the study also had some limitations. We combined data sets from two imaging laboratories – eleven subjects, i.e. one third of the total number, was derived from the Eggers study (Eggers et al., 2009). However, all subjects were examined on identical PET scanners, using nearly identical methodology (FDG dose, time from injection to scan, reconstruction). The data from the two centers differed with respect to MRI instrumentation; whereas our center used a 3.0T magnet, the German center used a 1.5T magnet. However, we believe that

careful inspection and manual editing of the VOIs defined on each individual MRI scan should have minimized the potential error from this source. Needless to say, our results represent only one single study. Thus, replication of the results is needed to more conclusively demonstrate the robustness of the findings. Optimally, verification of true hypermetabolism should be sought using fully quantitative data. However, as reviewed in section 2, the inherent variance in quantitative data demands extraordinarily large sample sizes. Such studies are consequently very costly and resource demanding, and are unlikely to be conducted by any single imaging center, but rather arise from multi-centre collaborations.

9. MRI STUDIES IN PD

One well-known possible cause of a decreased cortical PET signal has nothing to do with disease-related perfusion or metabolism defects. This cause, termed collectively the partial volume effects (PVE), arises in part because each PET voxel contains several tissue types, i.e. grey matter, white matter, and cerebrospinal fluid. Two or even all three tissue classes can sometimes be included in a single voxel, depending on the scanner resolution. The recorded PET signal is therefore a conglomerate of signals derived from several types of tissue. Consequently, it is difficult to determine whether a hypometabolic voxel is caused by the presence of an unchanged volume of truly hypometabolic tissue (true hypometabolism), or by a decreased volume of normometabolic tissue (atrophy). Several investigators have developed different ways of partial volume correction (PVC), all of which involve the use of MRI data to correct the PET data (Rousset et al., 1998, Meltzer et al., 2000). A review of these methodological details is beyond the scope of the present review. While we did not apply PVC to our PET or SPECT data, the subject is considered in the present section.

PVC has been applied successfully to perfusion (Meltzer et al., 2000) and glucose metabolism (Yanase et al., 2005) PET studies of healthy aging. Both studies reported regional cortical decreases with healthy aging, which were resolved after PVC. The question remains whether the cortical hypoactivity reported in PD patients is fully or partly to be explained by cortical atrophy. Very few studies have investigated this issue. Firbank and colleagues (Firbank et al., 2003) performed PVC on SPECT perfusion PD data, and found that primarily the posterior perfusion deficits, i.e. occipital and parietal deficits, were not explained by concomitant atrophy. The authors used cerebellum normalization, which, based on our findings (**Figure 11**), is expected to reveal substantially less of the true disease-related changes than is data-driven normalization. We therefore predict that a re-analysis of this data-set with data-driven normalization would reveal a larger portion of cerebral cortex to be hypoperfused. Sadly, no PET study has yet investigated PVC with reference cluster normalized data.

Despite this deficiency, a number of stand-alone MRI studies have investigated the extent of cortical atrophy in PD. Several reviews were published recently (Dagher and Nagano-Saito, 2007, Seppi and Poewe, 2010). In brief, measurable atrophy has mainly been reported in moderate- to late-stage PD patients (Camicioli et al., 2003, Burton et al., 2004, Nagano-Saito et al., 2005, Ramirez-Ruiz et al., 2005, Summerfield et al., 2005, Tam et al., 2005, Beyer et al., 2007, Song et al., 2011), and here mostly in the cingulate gyrus, insula, and fronto-temporal regions. These studies were performed using visual inspection, VOI analyses, or voxel-based analyses such as voxel-based morphometry (VBM) (Ashburner and Friston, 2000). However, to our knowledge early stage patients were not examined prior to our study.

This motivated us to conduct an MRI study on the subset of our patients deemed to have early PD. Twenty-four PD patients were compared to 26 age-matched controls. We initially performed a VBM analysis, but this approach (Borghammer et al., 2010b) did not reveal significant differences (unpublished observation). This negative result prompted us to attempt a deformation-based morphometry (DBM) analysis, which have been proposed to be more sensitive than VBM (Ashburner et al., 1998). In short, the method examines the transformation fields derived from coregistration of the individual MRI scans to common space. Thereby, an estimation is obtained of significant regional expansions and contractions in one group compared to another. Contractions are mostly found in solid tissue regions, and are interpreted as tissue atrophy. Expansions are mostly located in sulci and ventricles, and are interpreted as arising from the secondary widening of sulci caused by tissue atrophy. In the present group comparison, we detected significant contractions only in a part of the left cerebellum (Figure 1 of (Borghammer et al., 2010b)). However, at a less stringent t-threshold ($t<0.01$) small clusters of contractions were observed in several central WM regions, and expansions in several sulci, including the frontal lobe, insula, lateral parieto-temporal, and lateral occipital lobe. A regression analysis of the DBM data vs. patient UPDRS scores revealed significant or nearly-significant expansions, mostly located in frontal sulci (Figure 2 of (Borghammer et al., 2010b)).

Recently, two additional MRI studies of early PD patients have appeared. One study utilized yet another MRI analysis strategy, known as a cortical thickness analysis (Tinaz et al., 2011). The authors reported localized decreases of cortical thickness in frontal and lateral occipital regions. The other study investigated only ventricular volumes, and found that inferior lateral ventricles, third, and fourth ventricles were significantly expanded in early PD patients with cognitive deficit, but not in cognitively intact PD patients (Dalaker et al., 2011).

In summary, the varying MRI methodologies and patient groups make a formal comparison of these results difficult. However, it seems safe to conclude that any atrophy present at early disease stages is probably not very pronounced. In relation to the PVE issue in PET studies, it therefore seems unlikely that atrophy can account for the patterns of widespread cortical hypoactivity in its entirety (**Figure 11B**). Nevertheless, based on the current evidence (or lack there of), it cannot be excluded that early cortical atrophy could contribute somewhat to the cortical signal loss.

10. DISCUSSION

A few more Words on Normalization Methods

In the present review, we have provided evidence that PD is probably characterized by more extensive cortical hypoperfusion and hypometabolism than previously believed. Moreover, this cortical deficit seems to be present already at early disease stages. This insight was gained by utilization of unbiased data normalization methods, in particular the reference cluster technique. Caution must always be observed when employing novel methodology. However, we provided validation of the reference cluster method in a series of simulation studies (Borghammer et al., 2009a). Indeed, to our knowledge the majority of previous studies, which aimed to validate other normalization methods, employed real data rather than simulations. This was the case for

GM ratio normalization (Fox et al., 1988), ANOVA normalization with the GM as a covariate (Friston et al., 1990), and the SSM method (Moeller et al., 1987, Rottenberg et al., 1987, Strother et al., 1995, Alexander et al., 1999, Carbon et al., 2003, Habeck et al., 2005). The use of real data can be problematic, since the ground truth is of necessity unknown. This point is excellently exemplified by PD, in which the presence of true hypermetabolism in widespread regions is controversial.

Other papers have aimed to compare several normalization methods, but these studies also exclusively employed real patient data (Arndt et al., 1996, Gullion et al., 1996). Although we note that the Andersson method was validated using phantom data (Andersson, 1997), the phantom simulated a cortical activition paradigme, i.e. a large magnitude increase in a small localized region. This type of data is probably very different from the effects of neurodegeneration, in which extensive regions may exhibit changes of a much lower magnitude. As such, the Andersson method has not been validated for use in patient group comparisons – except by us (Borghammer et al., 2009a), and we demonstrated that although the Andersson method is preferable to GM ratio normalization, it has poorer performance than ratio normalization to an unbiased VOI.

To our knowledge, our studies (Borghammer et al., 2008, Borghammer et al., 2009a, Borghammer et al., 2009c) were the first to examine effects of data normalization in simulated "patient data", i.e. data containing spatially extensive decreases of low magnitude. The fitness and generalizability of simulated data must always be considered with caution. On the other hand the ground truth is known with certainty. We contend that our simulations constitute a plausible imitation of real patient data, based on several reasons. First, the manipulated spatial patterns were derived from real patient data comparisons. Second, we used real CBF parametric maps to ensure that the data displayed realistic noise properties. Third, we find it implausible that the widespread patterns of cortical hypoactivity, which are uncontroversially reported at late-stage disease, should suddenly spring into existence, without being preceded by similar patterns (of lower magnitude) at earlier disease stages. Fourth, the fitness of our simulated pattern was recently supported by the largest quantitative perfusion study performed in PD patients in the past 16 years (Melzer et al., 2011). In summary, we argue that ratio normalization to an unbiased VOI and the reference cluster method are more suitable to disclose true physiological changes in disease entities such as PD and AD. In other words, a finding of relatively increased metabolism in normalized data is, through the use of this method, more likely to reflect true underlying increased metabolism in the absolute sense.

It must be recalled that GM normalization can perform remarkably well when used for purposes other than assigning real alterations in physiological activity. For instance, the PD related pattern derived by the SSM method is highly reproducible and specific for PD in both CBF and CMRglc data (Eidelberg et al., 1994, Moeller et al., 1999, Asanuma et al., 2005, Huang et al., 2007, Ma et al., 2007). The pattern has been used for differential diagnostics, and to investigate effects of levodopa treatment and deep brain stimulation (Feigin et al., 2001, Fukuda et al., 2001, Asanuma et al., 2006). These applications do not require that the detected patterns be physiologically meaningful, only that they are specific.

Physiological interpretation – Lewy Body deposition

Given that PD patients, even at early stage, exhibit widespread cortical hypoperfusion and hypometabolism, how can this knowledge relate to other known aspects of neuropathology? First, α-synuclein-containing Lewy Bodies (LB) and Lewy neurites (LN) is a defining feature of the α-synucleinopathies, including PD (Spillantini et al., 1997). A very influential hypothesis regarding the deposition of LBs was published by Braak and colleagues (Braak et al., 2003). Based on a large post-mortem data set, the authors hypothesized that LBs appear in a certain, ascending pattern – starting at the bottom of the brainstem. From here the pathology ascends, involving multiple brainstem nuclei and then reaching the substantia nigra at stage 3, which is hypothesized to coincide with the appearance of motor symptoms. During the following three stages LBs appear in the cerebrum, initially in the medial temporal lobe, and subsequently in the tertiary and secondary neocortex throughout the brain. Although there have been some controversies concerning the validity of the "ascending hypothesis" (Jellinger, 2008), there is little doubt the many PD patients display a significant burden of cortical LBs at autopsy – in a pattern corresponding to Braak stage 5 and 6.

From the perspective of the present review, it is interesting to note the similarity between regions of cortical hypoactivity and LB accumulation. Only rarely are LBs deposited in the primary cortical regions, i.e. the sensory-motor cortex, primary visual and auditory cortices (Braak et al., 2003). The SMA also seems to be spared. The characteristic sparing of CBF in the primary sensory-motor cortex and SMA is also seen in **Figure 11**. On the other hand, the medial occipital lobe was found to be hypoactive in our studies, and several previous studies (Bohnen et al., 1999, Van Laere et al., 2004, Kasama et al., 2005). Thus, although a certain overlap is present, the cortical patterns are not identical. Nevertheless, it is an intriguing possibility that these two phenomena may be causally related. The neuropathology in PD is known to involve mitochondrial dysfunction (Schapira et al., 1989), oxidative stress and excitotoxicity (Beal, 2004), apoptosis, and proteasomal dysfunction (McNaught and Olanow, 2006). These factors are certainly interrelated in several ways with glucose and energy metabolism in several ways, but the exact details of the relationships need to be worked out.

To clarify any causal link between LB deposition and cortical hypometabolism further, it would be mandatory to understand the temporal relationship, i.e. which comes first. This is not known at present. To make matters worse, other studies have demonstrated that the relationship between clinical severity and Braak stages is unreliable (Jellinger, 2008). In other words, some patients apparently exhibit only mild (or no) symptoms in the presence of massive LB pathology. So the causal relationship, if any, cannot be simple. We are not aware of any studies having investigated the relationship between in vivo energy metabolism and the magnitude of LB deposition. Such studies are obviously extremely difficult to carry out, since post mortem examination is required. As such, the clarification of these issues will probably have to await the development of novel in vivo methods of α-synuclein detection, preferably in the form of a PET tracer.

Neuropathology in Ascending Neurotransmitter Systems

The degeneration of dopaminergic neurons in the substantia nigra (SN) is the universally acknowledged hallmark of PD (Damier et al., 1999). However, PD is now known to be a "multi-system disorder", which is characterized by early degeneration of several subcortical neuronal systems. In addition to the substantia nigra, there is also a substantial dopaminergic neuron loss in the ventral tegmental area (VTA), which provide the major dopaminergic input to the meso-limbic and prefrontal regions (Uhl et al., 1985).

A number of non-dopaminergic elements contribute to the PD pathology. The nucleus basalis of Meynert (NBM) provides large parts of the brain with cholinergic innervation. Significant neuron loss has been repeatedly confirmed in this structure in PD (Chan-Palay, 1988, Kosaka et al., 1988, Yoshimura, 1988, Sudarsky et al., 1989, Mattila et al., 2001, Zarow et al., 2003), as in AD. The cholinergic neurons of the pedunculo-pontine nucleus (PPN) likewise display significant degeneration (Hirsch et al., 1987, Jellinger, 1988). A very severe noradrenergic neuron loss, perhaps even exceeding the loss of dopamine neurons in the SN, has been reported in the locus coeruleus (Gai et al., 1991, German et al., 1992, Jellinger, 2000, Zarow et al., 2003). Finally, the serotonergic neurons of the dorsal raphe nuclei, which provide most of the brain with serotonergic input, also undergo significant degeneration (Agid et al., 1990, Jellinger, 1991, Jellinger and Paulus, 1992, Frisina et al., 2009).

The consequences of slow progressive neurodegenerative depletion of these neuronal systems on the resting state cortical perfusion and metabolism in PD are unknown. However, many studies have investigated the metabolic effects of acute or subchronic activation of each of these systems in isolation. To summarize some of the key findings of such studies, stimulation of the dopaminergic system increases CBF both regionally and globally in both animals and man (Leenders et al., 1985). Chemical or electrical stimulation of the cholinergic neurons of the NBM induces widespread cerebral vasodilation in rats (Biesold et al., 1989, Lacombe et al., 1989). Similar activation of the serotonergic neurons of the raphe nuclei elicits regional and global CBF increases in rats (Cudennec et al., 1993, Underwood et al., 1995). Thus, these ascending systems generally seem to have an activating and/or vasodilatory effect on the cerebral cortex.

Therefore, it seems plausible that the substantial neuron loss observed in PD in these ascending systems could result in spatially extensive hypoactivity and hypoperfusion in the cortex, as suggested by our findings. Even in absence of cortical neuropathology per se. Presumably, several homeostatic mechanisms will initially serve to counter the detrimental effects of the cortical denervations. Nevertheless, it is reasonable to assume that cortical hypoactivity could be present even at the very earliest symptomatic disease stages. After all, it is a well-known fact that 50-60% of nigral dopamine neurons (and perhaps even more of the noradrenergic neurons) are already lost when motor symptoms first appear (Schapira, 2009). The development of new PET tracers provides an opportunity to study some of these neurotransmitter systems. Interestingly, a recent PET study (Shimada et al., 2009) demonstrated decreased cortical acetylcholine esterase activity in early PD patients in a pattern quite similar to our reported patterns of hypometabolism. In summary, we hypothesize that the extensive cortical hypoactivity depicted in **Figure 11** may be a direct consequence of monoaminergic and cholinergic deafferentiation due to the severe degeneration of the respective subcortical nuclei.

The External Pallidum

In the high-resolution PET study (Borghammer et al., 2012), we provided evidence that the external pallidum probably displays real hypermetabolism in medication-fasting PD patients. The internal pallidum, VA/VL thalamic nuclei and putamen displayed relative hypermetabolism at a lower significance threshold. Thus, it is more doubtful (but still plausible) that these structures are truly hypermetabolic in PD. As reviewed in section 5, this also agrees with evidence from animal models of parkinsonism, wherein hypermetabolism in these structures is less consistently reported. These findings may be of some importance, since they demonstrate important similarities in the metabolic perturbation of the dopamine-depleted basal ganglia circuitry between PD patients and animal models of PD. This similarity is often taken for granted, but it has, we argue, never been formally demonstrated.

The present findings should also raise some more general questions about the neurobiology of the basal ganglia. In particular, what is so special about the external pallidum? Detailed and comprehensive models have been developed to explain the physiological activity of components of the parkinsonian basal ganglia (Alexander et al., 1990, Mink, 2003, Obeso et al., 2008). None of these models, however, predict that we should expect the highest magnitude of hypermetabolism in the external pallidum. As such, it seems that our knowledge of the parkinsonian basal ganglia circuitry is incomplete. More studies and perhaps a new explanatory framework will be needed if we are to gain a more detailed understanding of these observations.

Conclusion

Data normalization is commonly employed in perfusion and metabolism PET studies of Parkinson's disease (PD) and other disorders. Ratio normalization to the global mean (GM) is the most commonly used procedure. Its proper use requires, however, that no between-group differences exist in the GM. In a formal meta-analysis of the quantitative literature in PD (Borghammer et al., 2010a), we demonstrated that global levels of perfusion and metabolism are probably decreased in PD, even if undetected in many of the individual studies due to insufficient sample sizes. The use of GM normalization is therefore invalid.

A series of simulation studies were performed (Borghammer et al., 2008, Borghammer et al., 2009a, Borghammer et al., 2009b, Borghammer et al., 2009c), in which a simulated patient group was compared to control subjects. It emerged that when the patient group displays low-magnitude decreases in spatially extensive cortical regions, a subsequent GM normalized analysis is invariably biased (Borghammer et al., 2009c). Unchanged regions then appear hyperactive, whereas only a minor part of the true signal (i.e. cortical decreases) is recovered. Importantly, this bias occurs even when no detectable differences are present in the GM values, this due to inherent biological and methodological noise in the data. The mechanism of biased GM normalization explains why subcortical hypermetabolism in human PD has only ever been reported in GM normalized PET and SPECT studies, but never in fully quantitative studies and cerebellum-normalized studies. The simulation studies also determined that ratio normalization to an unbiased region, i.e. a region spared by the disease processes, performs better than GM normalization (Borghammer et al., 2009c). The best performance was obtained by a recently developed data-driven normalization approach known as reference cluster normalization. Using this method nearly the entire pattern of cortical hypoperfusion was recovered in the simulated data (Borghammer et al., 2009a).

The alternative normalization strategies were applied to several real-data comparisons of PD patients to age-matched controls (Borghammer et al., 2010a, Borghammer et al., 2012). When ratio-normalization to white matter and central cerebellum was used, and particularly when the reference cluster normalization was employed a widespread pattern of cortical hypoperfusion and hypometabolism was detected. The pattern was nearly identical across four groups of patients, and was seen even at early disease stages. Thus, the extent of cortical hypometabolism and

hypoperfusion may be more extensive than previously believed, and may be present at an earlier stage.

Finally, to investigate similarities in small subcortical structures between human PD and animal models, a study was performed using a brain-dedicated high-resolution PET scanner (Borghammer et al., 2012). This is the only available PET camera with sufficient resolution to allow valid investigation of the small nuclei of the basal ganglia, which have been implicated by the animal evidence. Furthermore, normalization of the new data was performed using the unbiased methods summarized above. In that study, the most significant level of subcortical hypermetabolism in PD was found in the external pallidum, which is in excellent agreement with the animal literature.

ABBREVATIONS

2DG	2-Deoxyglucose
6-OHDA	6-Hydroxydopamine
AD	Alzheimer's disease
ANOVA	Analysis of variance
CBF	Cerebral blood flow
CM	Centromedian nucleus of the thalamus
$CMRO_2$	Cerebral metabolic rate of oxygen
CMRglc	Cerebral metabolic rate of glucose
COV	Coefficient of variance (SD/mean)
FDG	6-Fluoro-deoxyglucose
FWHM	Full-width-at-half-maximum
GM	Global Mean
GPe	External pallidum
GPi	Internal pallidum
H&Y	Hoehn and Yahr scale
HE	Hepatic encephalopathy
L-dopa	Levodopa
MNI	Montreal Neurological Institute
MPTP	1-Methyl-4-phenyl-1,2,3,6-tetrahydropyridine
MRI	Magnet resonance Imagining
OEF	Oxygen extraction fraction
PD	Parkinson's disease
PET	Positron emission tomography
Pf	Parafascicular nucleus of the thalamus
PPN	Pedunculopontine nucleus
PVC	Partial volume correction
PVE	Partial volume effect
SD	Standard deviation
SMA	Supplementary motor area
SPECT	Single photon emission computed tomography
SPM	Statistical parametric mapping
SSM	Scaled subprofile model
STN	Subthalamic nucleus
TAL	Talairach coordinate system
UPDRS	Unified Parkinson's disease rating scale pt. III
VA	Ventral-anterior thalamic nucleus
VL	Ventral-lateral thalamic nucleus
VOI	Volume of interest
WB	Whole brain
WM	White matter

REFERENCES

Aarsland, D. & Kurz, M. W. 2010. The epidemiology of dementia associated with Parkinson's disease. *Brain Pathology,* **20,** 633-9.

Abe, Y., Kachi, T., Kato, T., Arahata, Y., Yamada, T., Washimi, Y., Iwai, K., et. al. 2003. Occipital hypoperfusion in Parkinson's disease without dementia: correlation to impaired cortical visual processing. *J Neurol Neurosurg Psychiatry,* **74,** 419-22.

Agid, Y., Graybiel, A. M., Ruberg, M., Hirsch, E., Blin, J., Dubois, B. & Javoy-Agid, F. 1990. The efficacy of levodopa treatment declines in the course of Parkinson's disease: do nondopaminergic lesions play a role? *Adv Neurol,* **53,** 83-100.

Agniel, A., Celsis, P., Viallard, G., Montastruc, J. L., Rascol, O., Demonet, J. F., Marc-Vergnes, J. P. & Rascol, A. 1991. Cognition and cerebral blood flow in lateralised parkinsonism: lack of functional lateral asymmetries. *J Neurol Neurosurg Psychiatry,* **54,** 783-6.

Ahl, B., Weissenborn, K., van den Hoff, J., Fischer-Wasels, D., Kostler, H., Hecker, H. & Burchert, W. 2004. Regional differences in cerebral blood flow and cerebral ammonia metabolism in patients with cirrhosis. *Hepatology,* **40,** 73-9.

Alavi, A., Smith, R. & Duncan, D. 1994. What are the sources of error in measuring and calculating cerebral metabolic rates with fluorine-18-fluorodeoxyglucose and PET? *J Nucl Med,* **35,** 1466-70.

Alexander, G. E., Crutcher, M. D. & DeLong, M. R. 1990. Basal ganglia-thalamocortical circuits: parallel substrates for motor, oculomotor, "prefrontal" and "limbic" functions. *Prog Brain Res,* **85,** 119-46.

Alexander, G. E., Mentis, M. J., Van Horn, J. D., Grady, C. L., Berman, K. F., Furey, M. L., Pietrini, P., Rapoport, S. I., Schapiro, M. B. & Moeller, J. R. 1999. Individual differences in PET activation of object perception and attention systems predict face matching accuracy. *Neuroreport,* **10,** 1965-71.

Andersson, J. L. 1997. How to estimate global activity independent of changes in local activity. *Neuroimage,* **6,** 237-44.

Antonini, A., De Notaris, R., Benti, R., De Gaspari, D. & Pezzoli, G. 2001. Perfusion ECD/SPECT in the characterization of cognitive deficits in Parkinson's disease. *Neurol Sci,* **22,** 45-6.

Arahata, Y., Hirayama, M., Ieda, T., Koike, Y., Kato, T., Tadokoro, M., Ikeda, M., Ito, K. & Sobue, G. 1999. Parieto-occipital glucose hypometabolism in Parkinson's disease with autonomic failure. *J Neurol Sci,* **163,** 119-26.

Arndt, S., Cizadlo, T., O'Leary, D., Gold, S. & Andreasen, N. C. 1996. Normalizing counts and cerebral blood flow intensity in functional imaging studies of the human brain. *Neuroimage,* **3,** 175-84.

Arndt, S., Cohen, G., Alliger, R. J., Swayze, V. W., 2nd & Andreasen, N. C. 1991. Problems with ratio and proportion measures of imaged cerebral structures. *Psychiatry Res,* **40,** 79-89.

Asanuma, K., Ma, Y., Huang, C., Carbon-Correll, M., Edwards, C., Raymond, D., Bressman, S. B., Moeller, J. R. & Eidelberg, D. 2005. The metabolic pathology of dopa-responsive dystonia. *Ann Neurol,* **57,** 596-600.

Asanuma, K., Tang, C., Ma, Y., Dhawan, V., Mattis, P., Edwards, C., Kaplitt, M. G., Feigin, A. & Eidelberg, D. 2006. Network modulation in the treatment of Parkinson's disease. *Brain,* **129,** 2667-78.

Ashburner, J. & Friston, K. J. 2000. Voxel-based morphometry--the methods. *Neuroimage,* **11,** 805-21.

Ashburner, J., Hutton, C., Frackowiak, R., Johnsrude, I., Price, C. & Friston, K. 1998. Identifying global anatomical differences: deformation-based morphometry. *Hum Brain Mapp,* **6,** 348-57.

Attwell, D. & Iadecola, C. 2002. The neural basis of functional brain imaging signals. *Trends Neurosci,* **25,** 621-5.

Bailey, D. L., Townsend, D., Valk, P. E. & Maisey, M. N. 2005. *Positron Emission Tomography: Basic Sciences*, Springer.

Beal, M. F. 2004. Mitochondrial dysfunction and oxidative damage in Alzheimer's and Parkinson's diseases and coenzyme Q10 as a potential treatment. *J Bioenerg Biomembr,* **36,** 381-6.

Ben-Shachar, D., Bonne, O., Chisin, R., Klein, E., Lester, H., Aharon-Peretz, J., Yona, I. & Freedman, N. 2007. Cerebral glucose utilization and platelet mitochondrial complex I activity in schizophrenia: A FDG-PET study. *Prog Neuropsychopharmacol Biol Psychiatry,* **31,** 807-13.

Berding, G., Odin, P., Brooks, D. J., Nikkhah, G., Matthies, C., Peschel, T., Shing, M., Kolbe, H., van Den Hoff, J., Fricke, H., Dengler, R., Samii, M. & Knapp, W. H. 2001. Resting regional cerebral glucose metabolism in advanced Parkinson's disease studied in the off and on conditions with [(18)F]FDG-PET. *Mov Disord,* **16,** 1014-22.

Bes, A., Guell, A., Fabre, N., Dupui, P., Victor, G. & Geraud, G. 1983. Cerebral blood flow studied by Xenon-133 inhalation technique in parkinsonism: loss of hyperfrontal pattern. *J Cereb Blood Flow Metab,* **3,** 33-7.

Beyer, M. K., Janvin, C. C., Larsen, J. P. & Aarsland, D. 2007. A magnetic resonance imaging study of patients with Parkinson's disease with mild cognitive impairment and dementia using voxel-based morphometry. *J Neurol Neurosurg Psychiatry,* **78,** 254-9.

Bezard, E., Crossman, A. R., Gross, C. E. & Brotchie, J. M. 2001. Structures outside the basal ganglia may compensate for dopamine loss in the presymptomatic stages of Parkinson's disease. *Faseb J,* **15,** 1092-4.

Biesold, D., Inanami, O., Sato, A. & Sato, Y. 1989. Stimulation of the nucleus basalis of Meynert increases cerebral cortical blood flow in rats. *Neurosci Lett,* **98,** 39-44.

Bohnen, N. I., Minoshima, S., Giordani, B., Frey, K. A. & Kuhl, D. E. 1999. Motor correlates of occipital glucose hypometabolism in Parkinson's disease without dementia. *Neurology,* **52,** 541-6.

Borghammer, P. 2008. *Perfusion and Metabolism PET studies in Parkinson's Disease,* Aarhus, Aarhus University Press.

Borghammer, P., Aanerud, J. & Gjedde, A. 2009a. Data-driven intensity normalization of PET group comparison studies is superior to global mean normalization. *Neuroimage,* **46,** 981-8.

Borghammer, P., Chakravarty, M., Jonsdottir, K. Y., Sato, N., Matsuda, H., Ito, K., Arahata, Y., Kato, T. & Gjedde, A. 2010. Cortical hypometabolism and hypoperfusion in Parkinson's disease is extensive: probably even at early disease stages. *Brain Struct Funct,* **214,** 303-17.

Borghammer, P., Cumming, P., Aanerud, J., Forster, S. & Gjedde, A. 2009b. Subcortical elevation of metabolism in Parkinson's disease--a critical reappraisal in the context of global mean normalization. *Neuroimage,* **47,** 1514-21.

Borghammer, P., Cumming, P., Aanerud, J. & Gjedde, A. 2009c. Artefactual subcortical hyperperfusion in PET studies normalized to global mean: lessons from Parkinson's disease. *Neuroimage,* **45,** 249-57.

Borghammer, P., Hansen, S. B., Eggers, C., Chakravarty, M., Vang, K., Aanerud, J., Hilker, R., Heiss, W. D., Rodell, A., Munk, O. L., Keator, D. & Gjedde, A. 2012. Glucose metabolism in small subcortical structures in Parkinson's disease. *Acta Neurologica Scandinavica,* **125,** 303-310.

Borghammer, P., Jonsdottir, K. Y., Cumming, P., Ostergaard, K., Vang, K., Ashkanian, M., Vafaee, M., Iversen, P. & Gjedde, A. 2008. Normalization in PET group comparison studies--the importance of a valid reference region. *Neuroimage,* **40,** 529-40.

Borghammer, P., Ostergaard, K., Cumming, P., Gjedde, A., Rodell, A., Hall, N. & Chakravarty, M. M. 2009d. A deformation-based morphometry study of patients with early-stage Parkinson's disease. *European Journal of Neurology*.

Braak, H., Del Tredici, K., Rub, U., de Vos, R. A., Jansen Steur, E. N. & Braak, E. 2003. Staging of brain pathology related to sporadic Parkinson's disease. *Neurobiol Aging,* **24,** 197-211.

Brownell, A. L., Canales, K., Chen, Y. I., Jenkins, B. G., Owen, C., Livni, E., Yu, M., Cicchetti, F., Sanchez-Pernaute, R. & Isacson, O. 2003. Mapping of brain function after MPTP-induced neurotoxicity in a primate Parkinson's disease model. *Neuroimage,* **20,** 1064-75.

Buchsbaum, M. S., Buchsbaum, B. R., Hazlett, E. A., Haznedar, M. M., Newmark, R., Tang, C. Y. & Hof, P. R. 2007. Relative glucose metabolic rate higher in white matter in patients with schizophrenia. *Am J Psychiatry,* **164,** 1072-81.

Buchsbaum, M. S., Wu, J., DeLisi, L. E., Holcomb, H., Kessler, R., Johnson, J., King, A. C., Hazlett, E., Langston, K. & Post, R. M. 1986. Frontal cortex and basal ganglia metabolic rates assessed by positron emission tomography with [18F]2-deoxyglucose in affective illness. *J Affect Disord,* **10,** 137-52.

Burns, R. S., Chiueh, C. C., Markey, S. P., Ebert, M. H., Jacobowitz, D. M. & Kopin, I. J. 1983. A primate model of parkinsonism: selective destruction of dopaminergic neurons in the pars compacta of the substantia nigra by N-methyl-4-phenyl-1,2,3,6-tetrahydropyridine. *Proc Natl Acad Sci U S A,* **80,** 4546-50.

Burton, E. J., McKeith, I. G., Burn, D. J., Williams, E. D. & O'Brien, J. T. 2004. Cerebral atrophy in Parkinson's disease with and without dementia: a comparison with Alzheimer's disease, dementia with Lewy bodies and controls. *Brain,* **127,** 791-800.

Buzsaki, G., Kaila, K. & Raichle, M. 2007. Inhibition and brain work. *Neuron,* **56,** 771-83.

Camicioli, R., Moore, M. M., Kinney, A., Corbridge, E., Glassberg, K. & Kaye, J. A. 2003. Parkinson's disease is associated with hippocampal atrophy. *Mov Disord,* **18,** 784-90.

Cannon, J. R. & Greenamyre, J. T. 2010. Neurotoxic in vivo models of Parkinson's disease recent advances. *Prog Brain Res,* **184,** 17-33.

Carbon, M., Ghilardi, M. F., Feigin, A., Fukuda, M., Silvestri, G., Mentis, M. J., Ghez, C., Moeller, J. R. & Eidelberg, D. 2003. Learning networks in health and Parkinson's disease: reproducibility and treatment effects. *Hum Brain Mapp,* **19,** 197-211.

Carlson, J. D., Pearlstein, R. D., Buchholz, J., Iacono, R. P. & Maeda, G. 1999. Regional metabolic changes in the pedunculopontine nucleus of unilateral 6-hydroxydopamine Parkinson's model rats. *Brain Res,* **828,** 12-9.

Casteels, C., Lauwers, E., Bormans, G., Baekelandt, V. & Van Laere, K. 2007. Metabolic-dopaminergic mapping of the 6-hydroxydopamine rat model for Parkinson's disease. *Eur J Nucl Med Mol Imaging*.

Chan-Palay, V. 1988. Galanin hyperinnervates surviving neurons of the human basal nucleus of Meynert in dementias of Alzheimer's and Parkinson's disease: a hypothesis for the role of galanin in accentuating cholinergic dysfunction in dementia. *Journal of Comparative Neurology,* **273,** 543-57.

Choo, I. H., Lee, D. Y., Youn, J. C., Jhoo, J. H., Kim, K. W., Lee, D. S., Lee, J. S. & Woo, J. I. 2007. Topographic patterns of brain functional impairment progression according to clinical severity staging in 116 Alzheimer disease patients: FDG-PET study. *Alzheimer Dis Assoc Disord,* **21,** 77-84.

Cudennec, A., Bonvento, G., Duverger, D., Lacombe, P., Seylaz, J. & MacKenzie, E. T. 1993. Effects of dorsal raphe nucleus stimulation on cerebral blood flow and flow-metabolism coupling in the conscious rat. *Neuroscience,* **55,** 395-401.

Dagher, A. & Nagano-Saito, A. 2007. Functional and anatomical magnetic resonance imaging in Parkinson's disease. *Mol Imaging Biol,* **9,** 234-42.

Dalaker, T. O., Zivadinov, R., Ramasamy, D. P., Beyer, M. K., Alves, G., Bronnick, K. S., Tysnes, O. B., Aarsland, D. & Larsen, J. P. 2011. Ventricular enlargement and mild cognitive impairment in early Parkinson's disease. *Mov Disord,* **26,** 297-301.

Damier, P., Hirsch, E. C., Agid, Y. & Graybiel, A. M. 1999. The substantia nigra of the human brain. II. Patterns of loss of dopamine-containing neurons in Parkinson's disease. *Brain,* **122 (Pt 8),** 1437-48.

Dauvilliers, Y., Comte, F., Bayard, S., Carlander, B., Zanca, M. & Touchon, J. 2010. A brain PET study in patients with narcolepsy-cataplexy. *J Neurol Neurosurg Psychiatry,* **81,** 344-8.

de Jong, H. W., van Velden, F. H., Kloet, R. W., Buijs, F. L., Boellaard, R. & Lammertsma, A. A. 2007. Performance evaluation of the ECAT HRRT: an LSO-LYSO double layer high resolution, high sensitivity scanner. *Physics in Medicine and Biology,* **52,** 1505-26.

Defebvre, L., Lecouffe, P., Destee, A., Houdart, P. & Steinling, M. 1995. Tomographic measurements of regional cerebral blood flow in progressive supranuclear palsy and Parkinson's disease. *Acta Neurol Scand,* **92,** 235-41.

Derejko, M., Slawek, J., Wieczorek, D., Brockhuis, B., Dubaniewicz, M. & Lass, P. 2006. Regional cerebral blood flow in Parkinson's disease as an indicator of cognitive impairment. *Nucl Med Commun,* **27,** 945-51.

Desco, M., Gispert, J. D., Reig, S., Sanz, J., Pascau, J., Sarramea, F., Benito, C., Santos, A., Palomo, T. & Molina, V. 2003. Cerebral metabolic patterns in chronic and recent-onset schizophrenia. *Psychiatry Res,* **122,** 125-35.

Di Chiro, G. & Brooks, R. A. 1988. PET quantitation: blessing and curse. *J Nucl Med,* **29,** 1603-4.

Diamant, M., Harms, M. P., Immink, R. V., Van Lieshout, J. J. & Van Montfrans, G. A. 2002. Twenty-four-hour non-invasive monitoring of systemic haemodynamics and cerebral blood flow velocity in healthy humans. *Acta Physiol Scand,* **175,** 1-9.

Doty, R. L., Stern, M. B., Pfeiffer, C., Gollomp, S. M. & Hurtig, H. I. 1992. Bilateral olfactory dysfunction in early stage treated and untreated idiopathic Parkinson's disease. *J Neurol Neurosurg Psychiatry,* **55,** 138-42.

Dubois, A., Herard, A. S., Delatour, B., Hantraye, P., Bonvento, G., Dhenain, M. & Delzescaux, T. 2010. Detection by voxel-wise statistical analysis of significant changes in regional cerebral glucose uptake in an APP/PS1 transgenic mouse model of Alzheimer's disease. *Neuroimage,* **51,** 586-98.

Eberling, J. L., Richardson, B. C., Reed, B. R., Wolfe, N. & Jagust, W. J. 1994. Cortical glucose metabolism in Parkinson's disease without dementia. *Neurobiol Aging,* **15,** 329-35.

Eckert, T., Barnes, A., Dhawan, V., Frucht, S., Gordon, M. F., Feigin, A. S. & Eidelberg, D. 2005. FDG PET in the differential diagnosis of parkinsonian disorders. *Neuroimage,* **26,** 912-21.

Eckert, T., Van Laere, K., Tang, C., Lewis, D. E., Edwards, C., Santens, P. & Eidelberg, D. 2007. Quantification of Parkinson's disease-related network expression with ECD SPECT. *Eur J Nucl Med Mol Imaging,* **34,** 496-501.

Eggers, C., Hilker, R., Burghaus, L., Schumacher, B. & Heiss, W. D. 2009. High resolution positron emission tomography demonstrates basal ganglia dysfunction in early Parkinson's disease. *J Neurol Sci,* **276,** 27-30.

Eidelberg, D., Moeller, J. R., Antonini, A., Kazumata, K., Nakamura, T., Dhawan, V., Spetsieris, P., deLeon, D., Bressman, S. B. & Fahn, S. 1998. Functional brain networks in DYT1 dystonia. *Ann Neurol,* **44,** 303-12.

Eidelberg, D., Moeller, J. R., Dhawan, V., Sidtis, J. J., Ginos, J. Z., Strother, S. C., Cedarbaum, J., Greene, P., Fahn, S. & Rottenberg, D. A. 1990. The metabolic anatomy of Parkinson's disease: complementary [18F]fluorodeoxyglucose and [18F]fluorodopa positron emission tomographic studies. *Mov Disord,* **5,** 203-13.

Eidelberg, D., Moeller, J. R., Dhawan, V., Spetsieris, P., Takikawa, S., Ishikawa, T., Chaly, T., Robeson, W., Margouleff, D., Przedborski, S. & et al. 1994. The metabolic topography of parkinsonism. *J Cereb Blood Flow Metab,* **14,** 783-801.

Engler, H., Lundberg, P. O., Ekbom, K., Nennesmo, I., Nilsson, A., Bergstrom, M., Tsukada, H., Hartvig, P. & Langstrom, B. 2003. Multitracer study with positron emission tomography in Creutzfeldt-Jakob disease. *Eur J Nucl Med Mol Imaging,* **30,** 85-95.

Feigin, A., Antonini, A., Fukuda, M., De Notaris, R., Benti, R., Pezzoli, G., Mentis, M. J., Moeller, J. R. & Eidelberg, D. 2002. Tc-99m ethylene cysteinate dimer SPECT in the differential diagnosis of parkinsonism. *Mov Disord,* **17,** 1265-70.

Feigin, A., Fukuda, M., Dhawan, V., Przedborski, S., Jackson-Lewis, V., Mentis, M. J., Moeller, J. R. & Eidelberg, D. 2001. Metabolic correlates of levodopa response in Parkinson's disease. *Neurology,* **57,** 2083-8.

Feigin, A., Tang, C., Ma, Y., Mattis, P., Zgaljardic, D., Guttman, M., Paulsen, J. S., Dhawan, V. & Eidelberg, D. 2007. Thalamic metabolism and symptom onset in preclinical Huntington's disease. *Brain,* **130,** 2858-67.

Firbank, M. J., Colloby, S. J., Burn, D. J., McKeith, I. G. & O'Brien, J. T. 2003. Regional cerebral blood flow in Parkinson's disease with and without dementia. *Neuroimage,* **20,** 1309-19.

Firbank, M. J., He, J., Blamire, A. M., Singh, B., Danson, P., Kalaria, R. N. & O'Brien, J. T. 2011. Cerebral blood flow by arterial spin labeling in poststroke dementia. *Neurology,* **76,** 1478-84.

Fox, P. T., Mintun, M. A., Reiman, E. M. & Raichle, M. E. 1988. Enhanced detection of focal brain responses using intersubject averaging and change-distribution analysis of subtracted PET images. *J Cereb Blood Flow Metab,* **8,** 642-53.

Frisina, P. G., Haroutunian, V. & Libow, L. S. 2009. The neuropathological basis for depression in Parkinson's disease. *Parkinsonism Relat Disord,* **15,** 144-8.

Friston, K. J., Frith, C. D., Liddle, P. F., Dolan, R. J., Lammertsma, A. A. & Frackowiak, R. S. 1990. The relationship between global and local changes in PET scans. *J Cereb Blood Flow Metab,* **10,** 458-66.

Frucht, S. J., Trost, M., Ma, Y. & Eidelberg, D. 2004. The metabolic topography of posthypoxic myoclonus. *Neurology,* **62,** 1879-81.

Fukuda, M., Mentis, M. J., Ma, Y., Dhawan, V., Antonini, A., Lang, A. E., Lozano, A. M., Hammerstad, J., Lyons, K., Koller, W. C., Moeller, J. R. & Eidelberg, D. 2001. Networks mediating the clinical effects of pallidal brain stimulation for Parkinson's disease: a PET study of resting-state glucose metabolism. *Brain,* **124,** 1601-9.

Fukuyama, H., Ogawa, M., Yamauchi, H., Yamaguchi, S., Kimura, J., Yonekura, Y. & Konishi, J. 1994. Altered cerebral energy metabolism in Alzheimer's disease: a PET study. *J Nucl Med,* **35,** 1-6.

Gai, W. P., Halliday, G. M., Blumbergs, P. C., Geffen, L. B. & Blessing, W. W. 1991. Substance P-containing neurons in the mesopontine tegmentum are severely affected in Parkinson's disease. *Brain,* **114 (Pt 5),** 2253-67.

German, D. C., Manaye, K. F., White, C. L., 3rd, Woodward, D. J., McIntire, D. D., Smith, W. K., Kalaria, R. N. & Mann, D. M. 1992. Disease-specific patterns of locus coeruleus cell loss. *Ann Neurol,* **32,** 667-76.

Ghaemi, M., Raethjen, J., Hilker, R., Rudolf, J., Sobesky, J., Deuschl, G. & Heiss, W. D. 2002. Monosymptomatic resting tremor and Parkinson's disease: a multitracer positron emission tomographic study. *Mov Disord,* **17,** 782-8.

Gjedde, A., Marrett, S. & Vafaee, M. 2002. Oxidative and nonoxidative metabolism of excited neurons and astrocytes. *J Cereb Blood Flow Metab,* **22,** 1-14.

Globus, M., Mildworf, B. & Melamed, E. 1985. Cerebral blood flow and cognitive impairment in Parkinson's disease. *Neurology,* **35,** 1135-9.

Gnanalingham, K. K., Milkowski, N. A., Smith, L. A., Hunter, A. J., Jenner, P. & Marsden, C. D. 1995. Short and long-term changes in cerebral [14C]-2-deoxyglucose uptake in the MPTP-treated marmoset: relationship to locomotor activity. *J Neural Transm Gen Sect,* **101,** 65-82.

Gullion, C. M., Devous, M. D., Sr. & Rush, A. J. 1996. Effects of four normalizing methods on data analytic results in functional brain imaging. *Biol Psychiatry,* **40,** 1106-21.

Habeck, C., Foster, N. L., Perneczky, R., Kurz, A., Alexopoulos, P., Koeppe, R. A., Drzezga, A. & Stern, Y. 2008. Multivariate and univariate neuroimaging biomarkers of Alzheimer's disease. *Neuroimage,* **40,** 1503-15.

Habeck, C., Krakauer, J. W., Ghez, C., Sackeim, H. A., Eidelberg, D., Stern, Y. & Moeller, J. R. 2005. A new approach to spatial covariance modeling of functional brain imaging data: ordinal trend analysis. *Neural Comput,* **17,** 1602-45.

Habeck, C. G. 2010. Basics of multivariate analysis in neuroimaging data. *J Vis Exp,* **July 24;(41),** pii: 1988.

Herholz, K. 2010. Cerebral glucose metabolism in preclinical and prodromal Alzheimer's disease. *Expert Rev Neurother,* **10,** 1667-73.

Hirsch, E. C., Graybiel, A. M., Duyckaerts, C. & Javoy-Agid, F. 1987. Neuronal loss in the pedunculopontine tegmental nucleus in Parkinson disease and in progressive supranuclear palsy. *Proc Natl Acad Sci U S A,* **84,** 5976-80.

Hoffman, E. J., Huang, S. C. & Phelps, M. E. 1979. Quantitation in positron emission computed tomography: 1. Effect of object size. *J Comput Assist Tomogr,* **3,** 299-308.

Hosey, L. A., Thompson, J. L., Metman, L. V., van den Munckhof, P. & Braun, A. R. 2005. Temporal dynamics of cortical and subcortical responses to apomorphine in Parkinson disease: an H2(15)O PET study. *Clin Neuropharmacol,* **28,** 18-27.

Hosokai, Y., Nishio, Y., Hirayama, K., Takeda, A., Ishioka, T., Sawada, Y., Suzuki, K., Itoyama, Y., Takahashi, S., Fukuda, H. & Mori, E. 2009. Distinct patterns of regional cerebral glucose metabolism in Parkinson's disease with and without mild cognitive impairment. *Mov Disord,* **24,** 854-62.

Hu, M. T., Taylor-Robinson, S. D., Chaudhuri, K. R., Bell, J. D., Labbe, C., Cunningham, V. J., Koepp, M. J., Hammers, A., Morris, R. G., Turjanski, N. & Brooks, D. J. 2000. Cortical dysfunction in non-demented Parkinson's disease patients: a combined (31)P-MRS and (18)FDG-PET study. *Brain,* **123 (Pt 2),** 340-52.

Huang, C., Tang, C., Feigin, A., Lesser, M., Ma, Y., Pourfar, M., Dhawan, V. & Eidelberg, D. 2007. Changes in network activity with the progression of Parkinson's disease. *Brain,* **130,** 1834-46.

Hutchins, G. D., Holden, J. E., Koeppe, R. A., Halama, J. R., Gatley, S. J. & Nickles, R. J. 1984. Alternative approach to single-scan estimation of cerebral glucose metabolic rate using glucose analogs, with particular application to ischemia. *J Cereb Blood Flow Metab,* **4,** 35-40.

Hutchinson, M., Nakamura, T., Moeller, J. R., Antonini, A., Belakhlef, A., Dhawan, V. & Eidelberg, D. 2000. The metabolic topography of essential blepharospasm: a focal dystonia with general implications. *Neurology,* **55,** 673-7.

Ibaraki, M., Shinohara, Y., Nakamura, K., Miura, S., Kinoshita, F. & Kinoshita, T. 2010. Interindividual variations of cerebral blood flow, oxygen delivery, and metabolism in relation to hemoglobin concentration measured by positron emission tomography in humans. *J Cereb Blood Flow Metab,* **30,** 1296-305.

Imon, Y., Matsuda, H., Ogawa, M., Kogure, D. & Sunohara, N. 1999. SPECT image analysis using statistical parametric mapping in patients with Parkinson's disease. *J Nucl Med,* **40,** 1583-9.

Jagust, W. J., Reed, B. R., Martin, E. M., Eberling, J. L. & Nelson-Abbott, R. A. 1992. Cognitive function and regional cerebral blood flow in Parkinson's disease. *Brain,* **115 (Pt 2),** 521-37.

Jellinger, K. 1988. The pedunculopontine nucleus in Parkinson's disease, progressive supranuclear palsy and Alzheimer's disease. *J Neurol Neurosurg Psychiatry,* **51,** 540-3.

Jellinger, K. A. 1991. Pathology of Parkinson's disease. Changes other than the nigrostriatal pathway. *Molecular and Chemical Neuropathology,* **14,** 153-97.

Jellinger, K. A. 2000. Morphological substrates of mental dysfunction in Lewy body disease: an update. *J Neural Transm Suppl,* **59,** 185-212.

Jellinger, K. A. 2008. A critical reappraisal of current staging of Lewy-related pathology in human brain. *Acta Neuropathol,* **116,** 1-16.

Jellinger, K. A. & Paulus, W. 1992. Clinico-pathological correlations in Parkinson's disease. *Clinical Neurology and Neurosurgery,* **94 Suppl,** S86-8.

Jokinen, P., Scheinin, N., Aalto, S., Nagren, K., Savisto, N., Parkkola, R., Rokka, J., Haaparanta, M., Roytta, M. & Rinne, J. O. 2010. [(11)C]PIB-, [(18)F]FDG-PET and MRI imaging in patients with Parkinson's disease with and without dementia. *Parkinsonism Relat Disord,* **16,** 666-70.

Kalpouzos, G., Chetelat, G., Baron, J. C., Landeau, B., Mevel, K., Godeau, C., Barre, L., Constans, J. M., Viader, F., Eustache, F. & Desgranges, B. 2007. Voxel-based mapping of brain gray matter volume and glucose metabolism profiles in normal aging. *Neurobiol Aging*.

Kalpouzos, G., Chetelat, G., Baron, J. C., Landeau, B., Mevel, K., Godeau, C., Barre, L., Constans, J. M., Viader, F., Eustache, F. & Desgranges, B. 2009. Voxel-based mapping of brain gray matter volume and glucose metabolism profiles in normal aging. *Neurobiol Aging,* **30,** 112-24.

Kapitan, M., Ferrando, R., Dieguez, E., de Medina, O., Aljanati, R., Ventura, R., Amorin, I., Salinas, D., Langhain, M., Gioia, A., Cardoso, A., Lago, G. & Buzo, R. 2009. [Regional cerebral blood flow changes in Parkinson's disease: correlation with disease duration]. *Revista Espanola de Medicina Nuclear,* **28,** 114-20.

Karbe, H., Holthoff, V., Huber, M., Herholz, K., Wienhard, K., Wagner, R. & Heiss, W. D. 1992. Positron emission tomography in degenerative disorders of the dopaminergic system. *J Neural Transm Park Dis Dement Sect,* **4,** 121-30.

Kasama, S., Tachibana, H., Kawabata, K. & Yoshikawa, H. 2005. Cerebral blood flow in Parkinson's disease, dementia with Lewy bodies, and Alzheimer's disease according to three-dimensional stereotactic surface projection imaging. *Dement Geriatr Cogn Disord,* **19,** 266-75.

Kawabata, K., Tachibana, H. & Sugita, M. 1991. Cerebral blood flow and dementia in Parkinson's disease. *J Geriatr Psychiatry Neurol,* **4,** 194-203.

Kehagia, A. A., Barker, R. A. & Robbins, T. W. 2010. Neuropsychological and clinical heterogeneity of cognitive impairment and dementia in patients with Parkinson's disease. *Lancet Neurol,* **9,** 1200-13.

Kikuchi, A., Takeda, A., Kimpara, T., Nakagawa, M., Kawashima, R., Sugiura, M., Kinomura, S., Fukuda, H., Chida, K., Okita, N., Takase, S. & Itoyama, Y. 2001. Hypoperfusion in the supplementary motor area, dorsolateral prefrontal cortex and insular cortex in Parkinson's disease. *J Neurol Sci,* **193,** 29-36.

Kitamura, S., Ujike, T., Kuroki, S., Sakamoto, S., Soeda, T., Iio, M. & Terashi, A. 1988. [Cerebral blood flow and oxygen metabolism in patients with Parkinson's disease]. *No To Shinkei,* **40,** 979-85.

Kondo, S., Tanaka, M., Sun, X., Okamoto, K. & Hirai, S. 1994. [Cerebral blood flow and oxygen metabolism in patients with pure akinesia and progressive supranuclear palsy]. *Rinsho Shinkeigaku,* **34,** 531-7.

Kosaka, K., Tsuchiya, K. & Yoshimura, M. 1988. Lewy body disease with and without dementia: a clinicopathological study of 35 cases. *Clinical Neuropathology,* **7,** 299-305.

Kozlowski, M. R. & Marshall, J. F. 1980. Plasticity of [14C]2-deoxy-D-glucose incorporation into neostriatum and related structures in response to dopamine neuron damage and apomorphine replacement. *Brain Res,* **197,** 167-83.

Kozlowski, M. R. & Marshall, J. F. 1983. Recovery of function and basal ganglia [14C]2-deoxyglucose uptake after nigrostriatal injury. *Brain Res,* **259,** 237-48.

Kuhl, D. E., Metter, E. J. & Riege, W. H. 1984. Patterns of local cerebral glucose utilization determined in Parkinson's disease by the [18F]fluorodeoxyglucose method. *Ann Neurol,* **15,** 419-24.

Lacombe, P., Sercombe, R., Verrecchia, C., Philipson, V., MacKenzie, E. T. & Seylaz, J. 1989. Cortical blood flow increases induced by stimulation of the substantia innominata in the unanesthetized rat. *Brain Res,* **491,** 1-14.

Langston, J. W. 2006. The Parkinson's complex: parkinsonism is just the tip of the iceberg. *Ann Neurol,* **59,** 591-6.

Leenders, K. L., Perani, D., Lammertsma, A. A., Heather, J. D., Buckingham, P., Healy, M. J., Gibbs, J. M., Wise, R. J., Hatazawa, J., Herold, S. & et al. 1990. Cerebral blood flow, blood volume and oxygen utilization. Normal values and effect of age. *Brain,* **113 (Pt 1),** 27-47.

Leenders, K. L., Wolfson, L., Gibbs, J. M., Wise, R. J., Causon, R., Jones, T. & Legg, N. J. 1985. The effects of L-DOPA on regional cerebral blood flow and oxygen metabolism in patients with Parkinson's disease. *Brain,* **108 (Pt 1),** 171-91.

Lockwood, A. H., Yap, E. W., Rhoades, H. M. & Wong, W. H. 1991. Altered cerebral blood flow and glucose metabolism in patients with liver disease and minimal encephalopathy. *J Cereb Blood Flow Metab,* **11,** 331-6.

Lozza, C., Baron, J. C., Eidelberg, D., Mentis, M. J., Carbon, M. & Marie, R. M. 2004. Executive processes in Parkinson's disease: FDG-PET and network analysis. *Hum Brain Mapp,* **22,** 236-45.

Ma, Y., Tang, C., Moeller, J. R. & Eidelberg, D. 2009. Abnormal regional brain function in Parkinson's disease: truth or fiction? *Neuroimage,* **45,** 260-6.

Ma, Y., Tang, C., Spetsieris, P. G., Dhawan, V. & Eidelberg, D. 2007. Abnormal metabolic network activity in Parkinson's disease: test-retest reproducibility. *J Cereb Blood Flow Metab,* **27,** 597-605.

Markus, H. S., Costa, D. C. & Lees, A. J. 1994. HMPAO SPECT in Parkinson's disease before and after levodopa: correlation with dopaminergic responsiveness. *J Neurol Neurosurg Psychiatry,* **57,** 180-5.

Markus, H. S., Lees, A. J., Lennox, G., Marsden, C. D. & Costa, D. C. 1995. Patterns of regional cerebral blood flow in corticobasal degeneration studied using HMPAO SPECT; comparison with Parkinson's disease and normal controls. *Mov Disord,* **10,** 179-87.

Matsui, H., Udaka, F., Miyoshi, T., Hara, N., Tamura, A., Oda, M., Kubori, T., Nishinaka, K. & Kameyama, M. 2005. Brain perfusion differences between Parkinson's disease and multiple system atrophy with predominant parkinsonian features. *Parkinsonism Relat Disord,* **11,** 227-32.

Mattila, P. M., Roytta, M., Lonnberg, P., Marjamaki, P., Helenius, H. & Rinne, J. O. 2001. Choline acetytransferase activity and striatal dopamine receptors in Parkinson's disease in relation to cognitive impairment. *Acta Neuropathol,* **102,** 160-6.

McNaught, K. S. & Olanow, C. W. 2006. Protein aggregation in the pathogenesis of familial and sporadic Parkinson's disease. *Neurobiol Aging,* **27,** 530-45.

Meissner, W., Guigoni, C., Cirilli, L., Garret, M., Bioulac, B. H., Gross, C. E., Bezard, E. & Benazzouz, A. 2007. Impact of chronic subthalamic high-frequency stimulation on metabolic basal ganglia activity: a 2-deoxyglucose uptake and cytochrome oxidase mRNA study in a macaque model of Parkinson's disease. *Eur J Neurosci,* **25,** 1492-500.

Meltzer, C. C., Cantwell, M. N., Greer, P. J., Ben-Eliezer, D., Smith, G., Frank, G., Kaye, W. H., Houck, P. R. & Price, J. C. 2000. Does cerebral blood flow decline in healthy aging? A PET study with partial-volume correction. *J Nucl Med,* **41,** 1842-8.

Melzer, T. R., Watts, R., Macaskill, M. R., Pearson, J. F., Rueger, S., Pitcher, T. L., Livingston, L., Graham, C., Keenan, R., Shankaranarayanan, A., Alsop, D. C., Dalrymple-Alford, J. C. & Anderson, T. J. 2011. Arterial spin labelling reveals an abnormal cerebral perfusion pattern in Parkinson's disease. *Brain,* **134(Pt 3),** 845-55.

Mentis, M. J., McIntosh, A. R., Perrine, K., Dhawan, V., Berlin, B., Feigin, A., Edwards, C., Mattis, P. & Eidelberg, D. 2002. Relationships among the metabolic patterns that correlate with mnemonic, visuospatial, and mood symptoms in Parkinson's disease. *Am J Psychiatry,* **159,** 746-54.

Miletich, R. S., Quarantelli, M. & Di Chiro, G. 1994. Regional cerebral blood flow imaging with 99mTc-bicisate SPECT in asymmetric Parkinson's disease: studies with and without chronic drug therapy. *J Cereb Blood Flow Metab,* **14 Suppl 1,** S106-14.

Mink, J. W. 2003. The Basal Ganglia and involuntary movements: impaired inhibition of competing motor patterns. *Arch Neurol,* **60,** 1365-8.

Minoshima, S., Frey, K. A., Foster, N. L. & Kuhl, D. E. 1995. Preserved pontine glucose metabolism in Alzheimer disease: a reference region for functional brain image (PET) analysis. *J Comput Assist Tomogr,* **19,** 541-7.

Mitchell, I. J., Boyce, S., Sambrook, M. A. & Crossman, A. R. 1992. A 2-deoxyglucose study of the effects of dopamine agonists on the parkinsonian primate brain. Implications for the neural mechanisms that mediate dopamine agonist-induced dyskinesia. *Brain,* **115 (Pt 3),** 809-24.

Mitchell, I. J., Clarke, C. E., Boyce, S., Robertson, R. G., Peggs, D., Sambrook, M. A. & Crossman, A. R. 1989. Neural mechanisms underlying parkinsonian symptoms based upon regional uptake of 2-deoxyglucose in monkeys exposed to 1-methyl-4-phenyl-1,2,3,6-tetrahydropyridine. *Neuroscience,* **32,** 213-26.

Mitchell, I. J., Cross, A. J., Sambrook, M. A. & Crossman, A. R. 1986. Neural mechanisms mediating 1-methyl-4-phenyl-1,2,3, 6-tetrahydropyridine-induced parkinsonism in the monkey: relative contributions of the striatopallidal and striatonigral pathways as suggested by 2-deoxyglucose uptake. *Neurosci Lett,* **63,** 61-5.

Mito, Y., Yoshida, K., Yabe, I., Makino, K., Hirotani, M., Tashiro, K., Kikuchi, S. & Sasaki, H. 2005. Brain 3D-SSP SPECT analysis in dementia with Lewy bodies, Parkinson's disease with and without dementia, and Alzheimer's disease. *Clinical Neurology and Neurosurgery,* **107,** 396-403.

Miyazawa, N., Shinohara, T., Nagasaka, T. & Hayashi, M. 2010. Hypermetabolism in patients with dementia with Lewy bodies. *Clinical Nuclear Medicine,* **35,** 490-3.

Moeller, J. R., Ishikawa, T., Dhawan, V., Spetsieris, P., Mandel, F., Alexander, G. E., Grady, C., Pietrini, P. & Eidelberg, D. 1996. The metabolic topography of normal aging. *J Cereb Blood Flow Metab,* **16,** 385-98.

Moeller, J. R., Nakamura, T., Mentis, M. J., Dhawan, V., Spetsieres, P., Antonini, A., Missimer, J., Leenders, K. L. et.al. 1999. Reproducibility of regional metabolic covariance patterns: comparison of four populations. *J Nucl Med,* **40,** 1264-9.

Moeller, J. R., Strother, S. C., Sidtis, J. J. & Rottenberg, D. A. 1987. Scaled subprofile model: a statistical approach to the analysis of functional patterns in positron emission tomographic data. *J Cereb Blood Flow Metab,* **7,** 649-58.

Montastruc, J. L., Celsis, P., Agniel, A., Demonet, J. F., Doyon, B., Puel, M., Marc-Vergnes, J. P. & Rascol, A. 1987. Levodopa-induced regional cerebral blood flow changes in normal volunteers and patients with Parkinson's disease. Lack of correlation with clinical or neuropsychological improvements. *Mov Disord,* **2,** 279-89.

Mraovitch, S., Calando, Y., Onteniente, B., Peschanski, M. & Seylaz, J. 1993. Cerebrovascular and metabolic uncoupling in the caudate-putamen following unilateral lesion of the mesencephalic dopaminergic neurons in the rat. *Neurosci Lett,* **157,** 140-4.

Nagano-Saito, A., Kato, T., Arahata, Y., Washimi, Y., Nakamura, A., Abe, Y., Yamada, T., Iwai, K., Hatano, K., Kawasumi, Y., Kachi, T., Dagher, A. & Ito, K. 2004a. Cognitive- and motor-related regions in Parkinson's disease: FDOPA and FDG PET studies. *Neuroimage,* **22,** 553-61.

Nagano-Saito, A., Washimi, Y., Arahata, Y., Iwai, K., Kawatsu, S., Ito, K., Nakamura, A., Abe, Y., Yamada, T., Kato, T. & Kachi, T. 2004b. Visual hallucination in Parkinson's disease with FDG PET. *Mov Disord,* **19,** 801-6.

Nagano-Saito, A., Washimi, Y., Arahata, Y., Kachi, T., Lerch, J. P., Evans, A. C., Dagher, A. & Ito, K. 2005. Cerebral atrophy and its relation to cognitive impairment in Parkinson disease. *Neurology,* **64,** 224-9.

Nicholson, R. M., Kusne, Y., Nowak, L. A., LaFerla, F. M., Reiman, E. M. & Valla, J. 2010. Regional cerebral glucose uptake in the 3xTG model of Alzheimer's disease highlights common regional vulnerability across AD mouse models. *Brain Res,* **1347,** 179-85.

O'Carroll, R. E., Hayes, P. C., Ebmeier, K. P., Dougall, N., Murray, C., Best, J. J., Bouchier, I. A. & Goodwin, G. M. 1991. Regional cerebral blood flow and cognitive function in patients with chronic liver disease. *Lancet,* **337,** 1250-3.

Obeso, J. A., Marin, C., Rodriguez-Oroz, C., Blesa, J., Benitez-Temino, B., Mena-Segovia, J., Rodriguez, M. & Olanow, C. W. 2008. The basal ganglia in Parkinson's disease: current concepts and unexplained observations. *Ann Neurol,* **64 Suppl 2,** S30-46.

Osaki, Y., Morita, Y., Fukumoto, M., Akagi, N., Yoshida, S. & Doi, Y. 2005. Three-dimensional stereotactic surface projection SPECT analysis in Parkinson's disease with and without dementia. *Mov Disord,* **20,** 999-1005.

Otsuka, M., Ichiya, Y., Hosokawa, S., Kuwabara, Y., Tahara, T., Fukumura, T., Kato, M., Masuda, K. & Goto, I. 1991. Striatal blood flow, glucose metabolism and 18F-dopa uptake: difference in Parkinson's disease and atypical parkinsonism. *J Neurol Neurosurg Psychiatry,* **54,** 898-904.

Otsuka, M., Ichiya, Y., Kuwabara, Y., Hosokawa, S., Sasaki, M., Yoshida, T., Fukumura, T., Kato, M. & Masuda, K. 1996. Glucose metabolism in the cortical and subcortical brain structures in multiple system atrophy and Parkinson's disease: a positron emission tomographic study. *J Neurol Sci,* **144,** 77-83.

Palombo, E., Porrino, L. J., Bankiewicz, K. S., Crane, A. M., Sokoloff, L. & Kopin, I. J. 1990. Local cerebral glucose utilization in monkeys with hemiparkinsonism induced by intracarotid infusion of the neurotoxin MPTP. *J Neurosci,* **10,** 860-9.

Palombo, E., Porrino, L. J., Crane, A. M., Bankiewicz, K. S., Kopin, I. J. & Sokoloff, L. 1991. Cerebral metabolic effects of monoamine oxidase inhibition in normal and 1-methyl-4-phenyl-1,2,3,6-tetrahydropyridine acutely treated monkeys. *J Neurochem,* **56,** 1639-46.

Parkinson, J. 1817. *An essay on the shaking palsy.,* London, Whittingham and Rowland.

Peppard, R. F., Martin, W. R., Carr, G. D., Grochowski, E., Schulzer, M., Guttman, M., McGeer, P. L., Phillips, A. G., Tsui, J. K. & Calne, D. B. 1992. Cerebral glucose metabolism in Parkinson's disease with and without dementia. *Arch Neurol,* **49,** 1262-8.

Peran, P., Cherubini, A., Luccichenti, G., Hagberg, G., Demonet, J. F., Rascol, O., Celsis, P., Caltagirone, C., Spalletta, G. & Sabatini, U. 2009. Volume and iron content in basal ganglia and thalamus. *Human Brain Mapping,* **30,** 2667-75.

Perico, C. A., Skaf, C. R., Yamada, A., Duran, F., Buchpiguel, C. A., Castro, C. C., Soares, J. C. & Busatto, G. F. 2005. Relationship between regional cerebral blood flow and separate symptom clusters of major depression: a single photon emission computed tomography study using statistical parametric mapping. *Neuroscience Letters,* **384,** 265-70.

Perlmutter, J. S. & Raichle, M. E. 1985. Regional blood flow in hemiparkinsonism. *Neurology,* **35,** 1127-34.

Piao, Y. S., Mori, F., Hayashi, S., Tanji, K., Yoshimoto, M., Kakita, A., Wakabayashi, K. & Takahashi, H. 2003. Alpha-synuclein pathology affecting Bergmann glia of the cerebellum in patients with alpha-synucleinopathies. *Acta Neuropathol,* **105,** 403-9.

Piert, M., Koeppe, R. A., Giordani, B., Minoshima, S. & Kuhl, D. E. 1996. Determination of regional rate constants from dynamic FDG-PET studies in Parkinson's disease. *J Nucl Med,* **37,** 1115-22.

Pizzolato, G., Dam, M., Borsato, N., Saitta, B., Da Col, C., Perlotto, N., Zanco, P., Ferlin, G. & Battistin, L. 1988. [99mTc]-HM-PAO SPECT in Parkinson's disease. *J Cereb Blood Flow Metab,* **8,** S101-8.

Playford, E. D., Jenkins, I. H., Passingham, R. E., Nutt, J., Frackowiak, R. S. & Brooks, D. J. 1992. Impaired mesial frontal and putamen activation in Parkinson's disease: a positron emission tomography study. *Ann Neurol,* **32,** 151-61.

Porrino, L. J., Burns, R. S., Crane, A. M., Palombo, E., Kopin, I. J. & Sokoloff, L. 1987. Changes in local cerebral glucose utilization associated with Parkinson's syndrome induced by 1-methyl-4-phenyl-1,2,3,6-tetrahydropyridine (MPTP) in the primate. *Life Sci,* **40,** 1657-64.

Poston, K. L. & Eidelberg, D. 2010. FDG PET in the Evaluation of Parkinson's Disease. *PET Clin,* **5,** 55-64.

Pourfar, M., Feigin, A., Tang, C. C., Carbon-Correll, M., Bussa, M., Budman, C., Dhawan, V. & Eidelberg, D. 2011. Abnormal metabolic brain networks in Tourette syndrome. *Neurology,* **76,** 944-52.

Powers, W. J., Videen, T. O., Markham, J., Black, K. J., Golchin, N. & Perlmutter, J. S. 2008. Cerebral mitochondrial metabolism in early Parkinson's disease. *J Cereb Blood Flow Metab,* **28,** 1754-60.

Ramirez-Ruiz, B., Marti, M. J., Tolosa, E., Bartres-Faz, D., Summerfield, C., Salgado-Pineda, P., Gomez-Anson, B. & Junque, C. 2005. Longitudinal evaluation of cerebral morphological changes in Parkinson's disease with and without dementia. *J Neurol,* **252,** 1345-52.

Ramsay, S. C., Murphy, K., Shea, S. A., Friston, K. J., Lammertsma, A. A., Clark, J. C., Adams, L., Guz, A. & Frackowiak, R. S. 1993. Changes in global cerebral blood flow in humans: effect on regional cerebral blood flow during a neural activation task. *J Physiol,* **471,** 521-34.

Reed, L. J., Lasserson, D., Marsden, P., Stanhope, N., Stevens, T., Bello, F., Kingsley, D., Colchester, A. & Kopelman, M. D. 2003. FDG-PET findings in the Wernicke-Korsakoff syndrome. *Cortex,* **39,** 1027-45.

Rottenberg, D. A., Moeller, J. R., Strother, S. C., Sidtis, J. J., Navia, B. A., Dhawan, V., Ginos, J. Z. & Price, R. W. 1987. The metabolic pathology of the AIDS dementia complex. *Ann Neurol,* **22,** 700-6.

Rougemont, D., Baron, J. C., Collard, P., Bustany, P., Comar, D. & Agid, Y. 1984. Local cerebral glucose utilisation in treated and untreated patients with Parkinson's disease. *J Neurol Neurosurg Psychiatry,* **47,** 824-30.

Rousset, O. G., Ma, Y. & Evans, A. C. 1998. Correction for partial volume effects in PET: principle and validation. *J Nucl Med,* **39,** 904-11.

Sadowski, M., Pankiewicz, J., Scholtzova, H., Ji, Y., Quartermain, D., Jensen, C. H., Duff, K., Nixon, R. A., Gruen, R. J. & Wisniewski, T. 2004. Amyloid-beta deposition is associated with decreased hippocampal glucose metabolism and spatial memory impairment in APP/PS1 mice. *Journal of Neuropathology and Experimental Neurology,* **63,** 418-28.

Sagar, S. M. & Snodgrass, S. R. 1980. Effects of substantia nigra lesions on forebrain 2-deoxyglucose retention in the rat. *Brain Res,* **185,** 335-48.

Sasaki, M., Ichiya, Y., Hosokawa, S., Otsuka, M., Kuwabara, Y., Fukumura, T., Kato, M., Goto, I. & Masuda, K. 1992. Regional cerebral glucose metabolism in patients with Parkinson's disease with or without dementia. *Ann Nucl Med,* **6,** 241-6.

Sawada, H., Udaka, F., Kameyama, M., Seriu, N., Nishinaka, K., Shindou, K., Kodama, M., Nishitani, N. & Okumiya, K. 1992. SPECT findings in Parkinson's disease associated with dementia. *J Neurol Neurosurg Psychiatry,* **55,** 960-3.

Scarmeas, N., Habeck, C. G., Zarahn, E., Anderson, K. E., Park, A., Hilton, J., Pelton, G. H., Tabert, M. H., Honig, L. S., Moeller, J. R., Devanand, D. P. & Stern, Y. 2004. Covariance PET patterns in early Alzheimer's disease and subjects with cognitive impairment but no dementia: utility in group discrimination and correlations with functional performance. *Neuroimage,* **23,** 35-45.

Schapira, A. H. 2009. Neurobiology and treatment of Parkinson's disease. *Trends Pharmacol Sci,* **30,** 41-7.

Schapira, A. H., Cooper, J. M., Dexter, D., Jenner, P., Clark, J. B. & Marsden, C. D. 1989. Mitochondrial complex I deficiency in Parkinson's disease. *Lancet,* **1,** 1269.

Schwartz, W. J., Sharp, F. R., Gunn, R. H. & Evarts, E. V. 1976. Lesions of ascending dopaminergic pathways decrease forebrain glucose uptake. *Nature,* **261,** 155-7.

Schwartzman, R. J. & Alexander, G. M. 1985. Changes in the local cerebral metabolic rate for glucose in the 1-methyl-4-phenyl-1,2,3,6-tetrahydropyridine (MPTP) primate model of Parkinson's disease. *Brain Res,* **358,** 137-43.

Schwartzman, R. J., Alexander, G. M., Ferraro, T. N., Grothusen, J. R. & Stahl, S. M. 1988. Cerebral metabolism of parkinsonian primates 21 days after MPTP. *Exp Neurol,* **102,** 307-13.

Seppi, K. & Poewe, W. 2010. Brain magnetic resonance imaging techniques in the diagnosis of parkinsonian syndromes. *Neuroimaging Clinics of North America,* **20,** 29-55.

Shimada, H., Hirano, S., Shinotoh, H., Aotsuka, A., Sato, K., Tanaka, N., Ota, T., Asahina, M., Fukushi, K., Kuwabara, S., Hattori, T., Suhara, T. & Irie, T. 2009. Mapping of brain acetylcholinesterase alterations in Lewy body disease by PET. *Neurology*.

Sirotin, Y. B. & Das, A. 2009. Anticipatory haemodynamic signals in sensory cortex not predicted by local neuronal activity. *Nature,* **457,** 475-9.

Sokoloff, L., Reivich, M., Kennedy, C., Des Rosiers, M. H., Patlak, C. S., Pettigrew, K. D., Sakurada, O. & Shinohara, M. 1977. The [14C]deoxyglucose method for the measurement of local cerebral glucose utilization: theory, procedure, and normal values in the conscious and anesthetized albino rat. *J Neurochem,* **28,** 897-916.

Song, S. K., Lee, J. E., Park, H. J., Sohn, Y. H., Lee, J. D. & Lee, P. H. 2011. The pattern of cortical atrophy in patients with Parkinson's disease according to cognitive status. *Mov Disord,* **26,** 289-96.

Soonawala, D., Amin, T., Ebmeier, K. P., Steele, J. D., Dougall, N. J., Best, J., Migneco, O., Nobili, F. & Scheidhauer, K. 2002. Statistical parametric mapping of (99m)Tc-HMPAO-SPECT images for the diagnosis of Alzheimer's disease: normalizing to cerebellar tracer uptake. *Neuroimage,* **17,** 1193-202.

Spampinato, U., Habert, M. O., Mas, J. L., Bourdel, M. C., Ziegler, M., de Recondo, J., Askienazy, S. & Rondot, P. 1991. (99mTc)-HM-PAO SPECT and cognitive impairment in Parkinson's disease: a comparison with dementia of the Alzheimer type. *J Neurol Neurosurg Psychiatry,* **54,** 787-92.

Spetsieris, P., Ma, Y., Dhawan, V., Moeller, J. R. & Eidelberg, D. 2006. Highly automated computer-aided diagnosis of neurological disorders using functional brain imaging. *Proc SPIE: Med Imag,* **6144,** 5M1-12.

Spetsieris, P. G., Ma, Y., Dhawan, V. & Eidelberg, D. 2009. Differential diagnosis of parkinsonian syndromes using PCA-based functional imaging features. *Neuroimage,* **45,** 1241-52.

Spillantini, M. G., Schmidt, M. L., Lee, V. M., Trojanowski, J. Q., Jakes, R. & Goedert, M. 1997. Alpha-synuclein in Lewy bodies. *Nature,* **388,** 839-40.

Strother, S. C., Anderson, J. R., Schaper, K. A., Sidtis, J. J., et al. 1995. Principal component analysis and the scaled subprofile model compared to intersubject averaging and statistical parametric mapping: I. "Functional connectivity" of the human motor system studied with [15O]water PET. *J Cereb Blood Flow Metab,* **15,** 738-53.

Sudarsky, L., Morris, J., Romero, J. & Walshe, T. M. 1989. Dementia in Parkinson's disease: the problem of clinicopathological correlation. *Journal of Neuropsychiatry and Clinical Neurosciences,* **1,** 159-66.

Summerfield, C., Junque, C., Tolosa, E., Salgado-Pineda, P., Gomez-Anson, B., Marti, M. J., Pastor, P., Ramirez-Ruiz, B. & Mercader, J. 2005. Structural brain changes in Parkinson disease with dementia: a voxel-based morphometry study. *Arch Neurol,* **62,** 281-5.

Tachibana, H., Tomino, Y., Kawabata, K., Sugita, M. & Fukuchi, M. 1995. Twelve-month follow-up study of regional cerebral blood flow in Parkinson's disease. *Dementia,* **6,** 89-93.

Talairach, J. & Tournoux, P. 1988. *Co-planar stereotaxic atlas of the human brain.,* New York, Thieme Verlag.

Tam, C. W., Burton, E. J., McKeith, I. G., Burn, D. J. & O'Brien, J. T. 2005. Temporal lobe atrophy on MRI in Parkinson disease with dementia: a comparison with Alzheimer disease and dementia with Lewy bodies. *Neurology,* **64,** 861-5.

Tinaz, S., Courtney, M. G. & Stern, C. E. 2011. Focal cortical and subcortical atrophy in early Parkinson's disease. *Mov Disord,* **26,** 436-41.

Trost, M., Carbon, M., Edwards, C., Ma, Y., Raymond, D., Mentis, M. J., Moeller, J. R., Bressman, S. B. & Eidelberg, D. 2002. Primary dystonia: is abnormal functional brain architecture linked to genotype? *Ann Neurol,* **52,** 853-6.

Trost, M., Su, S., Su, P., Yen, R. F., Tseng, H. M., Barnes, A., Ma, Y. & Eidelberg, D. 2006. Network modulation by the subthalamic nucleus in the treatment of Parkinson's disease. *Neuroimage,* **31,** 301-7.

Trugman, J. M. & Wooten, G. F. 1986. The effects of L-DOPA on regional cerebral glucose utilization in rats with unilateral lesions of the substantia nigra. *Brain Res,* **379,** 264-74.

Uhl, G. R., Hedreen, J. C. & Price, D. L. 1985. Parkinson's disease: loss of neurons from the ventral tegmental area contralateral to therapeutic surgical lesions. *Neurology,* **35,** 1215-8.

Underwood, M. D., Bakalian, M. J., Arango, V. & Mann, J. J. 1995. Effect of chemical stimulation of the dorsal raphe nucleus on cerebral blood flow in rat. *Neurosci Lett,* **199,** 228-30.

Uretsky, N. J. & Iversen, L. L. 1970. Effects of 6-hydroxydopamine on catecholamine containing neurones in the rat brain. *J Neurochem,* **17,** 269-78.

Valk, P. E., Bailey, D. L., Townsend, D. W. & Maisey, M. N. 2003. *Positron Emission Tomography - Basic Science and Clinical Applications,* London, Springer.

Van Laere, K., Santens, P., Bosman, T., De Reuck, J., Mortelmans, L. & Dierckx, R. 2004. Statistical parametric mapping of (99m)Tc-ECD SPECT in idiopathic Parkinson's disease and multiple system atrophy with predominant parkinsonian features: correlation with clinical parameters. *J Nucl Med,* **45,** 933-42.

Vander Borght, T., Minoshima, S., Giordani, B., Foster, N. L., Frey, K. A., Berent, S., Albin, R. L., Koeppe, R. A. & Kuhl, D. E. 1997. Cerebral metabolic differences in Parkinson's and Alzheimer's diseases matched for dementia severity. *J Nucl Med,* **38,** 797-802.

Wang, G. J., Volkow, N. D., Wolf, A. P., Brodie, J. D. & Hitzemann, R. J. 1994. Intersubject variability of brain glucose metabolic measurements in young normal males. *J Nucl Med,* **35,** 1457-66.

Wang, S. J., Liu, R. S., Liu, H. C., Lin, K. N., Shan, D. E., Liao, K. K., Fuh, J. L. & Lee, L. S. 1993. Technetium-99m hexamethylpropylene amine oxime single photon emission tomography of the brain in early Parkinson's disease: correlation with dementia and lateralization. *Eur J Nucl Med,* **20,** 339-44.

Williams, D. S., Detre, J. A., Leigh, J. S. & Koretsky, A. P. 1992. Magnetic resonance imaging of perfusion using spin inversion of arterial water. *Proc Natl Acad Sci U S A,* **89,** 212-6.

Wisniewski, T. & Sigurdsson, E. M. 2010. Murine models of Alzheimer's disease and their use in developing immunotherapies. *Biochimica et Biophysica Acta,* **1802,** 847-59.

Wolfson, L. I., Leenders, K. L., Brown, L. L. & Jones, T. 1985. Alterations of regional cerebral blood flow and oxygen metabolism in Parkinson's disease. *Neurology,* **35,** 1399-405.

Wooten, G. F. & Collins, R. C. 1981. Metabolic effects of unilateral lesion of the substantia nigra. *J Neurosci,* **1,** 285-91.

Wooten, G. F. & Collins, R. C. 1983. Effects of dopaminergic stimulation on functional brain metabolism in rats with unilateral substantia nigra lesions. *Brain Res,* **263,** 267-75.

Yakushev, I., Hammers, A., Fellgiebel, A., Schmidtmann, I., Scheurich, A., Buchholz, H. G., Peters, J., Bartenstein, P., Lieb, K. & Schreckenberger, M. 2009. SPM-based count normalization provides excellent discrimination of mild Alzheimer's disease and amnestic mild cognitive impairment from healthy aging. *Neuroimage,* **44,** 43-50.

Yanase, D., Matsunari, I., Yajima, K., Chen, W., Fujikawa, A., Nishimura, S., Matsuda, H. & Yamada, M. 2005. Brain FDG PET study of normal aging in Japanese: effect of atrophy correction. *Eur J Nucl Med Mol Imaging,* **32,** 794-805.

Yoshimura, M. 1988. Pathological basis for dementia in elderly patients with idiopathic Parkinson's disease. *European Neurology,* **28 Suppl 1,** 29-35.

Zarow, C., Lyness, S. A., Mortimer, J. A. & Chui, H. C. 2003. Neuronal loss is greater in the locus coeruleus than nucleus basalis and substantia nigra in Alzheimer and Parkinson diseases. *Arch Neurol,* **60,** 337-41.